Inorganic Chemistry

Article

pubs.acs.org/IC

Isotope Effects in ^{195}Pt NMR Spectroscopy: Unique $^{35/37}$Cl- and $^{16/18}$O-Resolved "Fingerprints" for All $[PtCl_{6-n}(OH)_n]^{2-}$ (n = 1−5) Anions in an Alkaline Solution and the Implications of the Trans Influence

Leon Engelbrecht, Pieter Murray, and Klaus R. Koch*

Department of Chemistry and Polymer Science, University of Stellenbosch, Post Bag X1, Matieland 7602, South Africa

Supporting Information

ABSTRACT: A detailed analysis of the intrinsic $^{1}\Delta^{195}Pt(^{37/35}Cl)$ and $^{1}\Delta^{195}Pt(^{18/16}O)$ isotope 128.8 MHz ^{195}Pt NMR profiles of the series of kinetically inert $[PtCl_{6-n}(OH)_n]^{2-}$ (n = 1−5) anions generated in strongly alkaline aqueous solutions shows that each ^{195}Pt NMR resonance of the $[Pt^{35/37}Cl_{6-n}(^{16/18}OH)_n]^{2-}$ (n = 1−5) anions is resolved only into $[(6 - n) + 1$ for n = 1−5$]$ $^{35/37}$Cl *isotopologues* at 293 K. Evidently, the greater trans influence of the hydroxido ligand in the order $OH^- > Cl^- > H_2O$ in $[PtCl_{6-n}(OH)_n]^{2-}$ (n = 1−5) complexes results in somewhat longer Pt−Cl bond displacements trans to the hydroxido ligands, resulting in the absence of isotopomer effects in the $[PtCl_{6-n}(OH)_n]^{2-}$ (n = 1−5) anions in contrast to that observed in the corresponding $[PtCl_{6-n}(H_2O)_n]^{(2-n)-}$ (n = 1−5) complexes. In suitably ^{18}O-enriched sodium hydroxide solutions, additional intrinsic $^{1}\Delta^{195}Pt(^{18/16}O)$ isotope effects are remarkably well-resolved into unique *isotopologue*- and *isotopomer*-based ^{195}Pt NMR profiles, ascribable to the higher trans influence of the OH^- ligand. The consequent significantly shorter Pt−OH bonds in these anions emphasize $^{16/18}$O isotopomer effects in the ^{195}Pt NMR peaks of $[Pt^{35/37}Cl_{6-n}(^{16/18}OH)_n]^{2-}$ (n = 1−5) for magnetically nonequivalent $^{16/18}$OH isotopomers statistically possible in some isotopologues. These ^{195}Pt NMR profiles constitute unique NMR "fingerprints", useful for the unambiguous assignment of the series of $[PtCl_{6-n}(OH)_n]^{2-}$ anions including their possible cis/trans/*fac*/*mer* stereoisomers in such solutions, without a need for accurate chemical shift measurements.

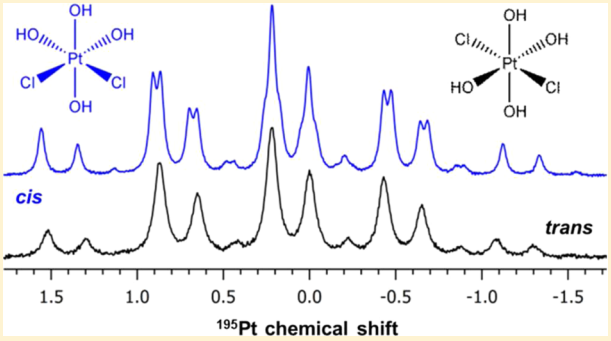

INTRODUCTION

Since the first accurate measurement of the positive magnetic moment[1] of the only stable magnetically active isotope of ^{195}Pt (I = $^{1}/_{2}$) at 33.83% natural abundance,[2] ^{195}Pt NMR spectroscopy has developed into a powerful spectroscopic tool for the study of the chemistry of countless platinum-containing compounds with oxidation states of platinum of 0, II, or IV in solution. This subject has been extensively reviewed in recent years.[3−6] The utility of ^{195}Pt NMR arises inter alia from its relatively high NMR receptivity, [2] with the very large known chemical shift $\delta(^{195}Pt)$ range exceeding 13000 ppm, which is extremely sensitive to the detailed structure of the platinum-containing molecules or complexes, as well as the generally large scalar (^{n}J) spin−spin coupling constants to other magnetically active nuclei.[3−6] These NMR parameters are generally excellent spectroscopic probes of the structure of the platinum-containing compound. In solution, the scalar spin−spin coupling constants between ^{195}Pt and other magnetically active nuclei can range from a few hertz to >140 kHz. The $^{1}J(^{195}Pt-^{205}Tl)$ coupling constant of 148 kHz observed in a dimeric platinum−thallium complex, $[\{Pt(ONO_2)(NH_3)_2(NHCOtBu)\}Tl(ONO_2)_2(MeOH)]$, is reported to be one of the largest known in solution.[7] Overall, the ^{195}Pt chemical shift range, reflecting the magnetic shielding of this nucleus within a given molecule in solution under defined conditions, is generally interpreted to result from several distinct shielding parameter contributions. These additive contributions may traditionally be formulated as $\sigma_{overall} = \sigma_d + \sigma_p + \sigma_{so} + \sigma_{other}$, where σ_d is the diamagnetic, σ_p the paramagnetic, and σ_{so} the relativistic spin−orbit coupling shielding contributions, including effects due to other "extraneous" factors upon shielding generally embodied in a σ_{other} shielding contribution term, respectively.[8−14] In this context, the experimentally observed sensitivity of $\delta(^{195}Pt)$/ppm to "other" factors (embodied in σ_{other}), such as the influence of the solvent,[15] temperature,[16] pressure, and isotope effects,[17,18,49] is documented in the literature, although the origin of such effects is still relatively poorly understood on a fundamental level.

In particular, isotope effects arising from the substitution of a heavier isotope for a lighter one of the same element usually

Received: December 8, 2014
Published: February 20, 2015

DOI: 10.1021/ic502901d
Inorg. Chem. 2015, 54, 2752−2764

directly bound to an NMR-active nucleus result in small but detectable changes in the magnetic shielding of the nucleus, particularly in high magnetic fields.[17−23] Typically, substitution of a lighter isotope for a heavier one results in increased magnetic shielding of the NMR-active nucleus in such a molecule (although not always),[20,22,23] while generally such isotope-induced shifts are approximately additive. Anet and Dekmezian[24] distinguish between *intrinsic* and *equilibrium* chemical-shift isotope effects, with the former relating to a single species on a single minimum energy surface and the latter involving more than one chemical species usually undergoing rapid chemical exchange of the isotopes between two or more sites, as is typically observed in $^{1}H/^{2}H$ exchange in ^{1}H NMR. While the majority of isotope effects in NMR have been examined in solution, intrinsic chemical-shift isotope effects have also been reported by Wasylishen et al.[25] in the solid state in a multinuclear NMR study.

As part of our interest in the high sensitivity of ^{195}Pt NMR spectroscopy for practical applications, we have explored the use of high-resolution ^{195}Pt NMR as an experimental spectroscopic tool for the understanding of chemical speciation and the solvation chemistry of platinum(IV) complexes in the domain of the refining and separations industry, at least in refinery process feed solutions, in which the concentrations of platinum in a hydrochloric acid solution are relatively high, ranging from 15 to 35 g/L. This was illustrated by our previous work using ^{195}Pt NMR for speciation of these complexes $[PtCl_{6-n}(H_2O)_n]^{(2-n)-}$ (n = 1−5), as well as highlighting the consequent influence on the efficiency of separation by ion exchange.[26−28] Recently, we demonstrated that the high-resolution 128 MHz ^{195}Pt NMR (at 14.1 T) signals of the series of deceptively simple aquated $[PtCl_{6-n}(H_2O)_n]^{(2-n)-}$ (n = 1−4) complexes in acidic halide-ion-rich aqueous solutions display remarkably well-resolved intrinsic isotope shifts in the ^{195}Pt NMR peak of these complexes, resulting in each separate ^{195}Pt NMR resonance being resolved into a unique NMR "fingerprint", suitable for the unambiguous identification of all of the complexes in the above series including their possible stereoisomers.[29,30] Generally, an intrinsic isotope shift for an NMR-active nucleus M bound to isotope X in a compound MX can be written as $^{n}\Delta M(^{m'/m}X)$ after the notation of Gombler[21] and Wasylishen et al.,[25] where m and m' are the mass numbers of the light and heavy isotopes of element X, respectively, bound to M, with n indicating the number of chemical bonds separating atoms M and X. Sadler et al. first reported the ^{195}Pt NMR peak of the octahedral $[PtCl_6]^{2-}$ anion in aqueous solution to be resolved into an asymmetric five-line pattern at a moderately high magnetic field (9.4 T).[17] The latter isotope profile of the ^{195}Pt resonance of $[Pt^{35}Cl_{6-n}{}^{37}Cl_n]^{2-}$ (n = 0−6) was ascribed to five of the seven possible "isotopomers", resulting from intrinsic $^{35/37}Cl$ isotope shifts of ca. −0.167 ppm per ^{37}Cl isotope, which, in fact, result from the *isotopologues* of $[Pt^{35}Cl_{6-n}{}^{37}Cl_n]^{2-}$ (n = 0−6). (There is some confusion in the use of the terms isotopomer and isotopologue in the NMR literature. The term isotopologue refers to molecules or complexes with a defined isotopic composition of their constituent atoms. Isotopomers are *isomers* of a given isotopologue having the same isotopic composition but differing in the relative positions of the isotopes within the molecule or complex.) Gröning and Elding[18] utilized $^{35/37}Cl$ and $^{16/18}O$ isotope effects in a study of the water-exchange rate in selected platinum(II) and platinum(IV) complexes in acidic solutions. Remarkably, we found that substitution of Cl^- ions by water in the series of aquated $[PtCl_{6-n}(H_2O)_n]^{(2-n)-}$ (n = 1−5)[29,30] or $[RhCl_{6-n}(H_2O)_n]^{3-n}$ (n = 0−4)[31] complexes results in an additional fine structure visible in the intrinsic $^{1}\Delta^{195}Pt(^{37/35}Cl)$ isotope profile of the $^{195}Pt/^{103}Rh$ NMR peaks in high magnetic fields, primarily as a result of magnetically nonequivalent isotopomers possible for some sets of isotopologues. This phenomenon appears to be general for kinetically inert chlorido/aqua complexes of these precious metals in aqueous solution, which in essence provides a means of unambiguous assignment of each chemical species, therefore obviating the common uncertainty in experimentally measured $\delta(^{195}Pt)$ or $\delta(^{103}Rh)$ chemical shifts.

In 1984, Goodfellow et al.[32] proposed a set of empirical assignment criteria for the ^{195}Pt NMR resonances of these species based only on relative chemical shift trends and intensities of the ^{195}Pt NMR resonances to identify the hydrolysis products of $[PtCl_6]^{2-}$ in strongly alkaline solutions. Subsequently, we extended the utility of such an empirical chemical-shift-trend approach, leading to the characterization of 33 previously unidentified complexes of the 52 possible $[PtCl_{6-m-n}Br_m(OH)_n]^{2-}$ (m, n = 0−6) complex anions in such solutions.[27] Although this methodology is useful for chemical speciation of closely related platinum(IV) complexes, it is very time-consuming and tedious, requiring careful control of the various extraneous effects to result in reliable ^{195}Pt NMR assignments.

We show here that the intrinsic $^{1}\Delta^{195}Pt(^{37/35}Cl)$ and $^{1}\Delta^{195}Pt(^{18/16}O)$ isotope profiles visible in each set of ^{195}Pt NMR resonances of the $[Pt^{35/37}Cl_{6-n}(^{16/18}OH)_n]^{2-}$ (n = 1−5) anions are reliable methoda for the unambiguous ^{195}Pt NMR assignments of the $[PtCl_{6-n}(OH)_n]^{2-}$ anions, without the need for accurate chemical shift measurements. In contrast to the corresponding set of aquated $[PtCl_{6-n}(H_2O)_n]^{(2-n)-}$ (n = 1−5) complexes in acid solutions, which show isotope $^{1}\Delta^{195}Pt(^{37/35}Cl)$ profiles resolved both at an *isotopologue* level and, in some cases, at the *isotopomer* level,[29,30] the ^{195}Pt NMR peaks of the $[PtCl_{6-n}(OH)_n]^{2-}$ (n = 1−5) anions show *only* intrinsic $^{1}\Delta^{195}Pt(^{37/35}Cl)$ isotope profiles resolved for each possible isotopologue of each anion under similar NMR experimental conditions. This remarkable and interesting difference in the intrinsic $^{1}\Delta^{195}Pt(^{37/35}Cl)$ isotope profiles of the ^{195}Pt NMR peaks of the $[Pt^{35/37}Cl_{6-n}(OH)_n]^{2-}$ (n = 1−5) anions, may at least qualitatively be ascribed to the higher trans influence of the hydroxido ligand in the order $OH^- > Cl^- > H_2O$,[33] resulting in slightly longer Pt−Cl bond displacements trans to the hydroxido ion in the octahedral $[Pt^{35/37}Cl_{6-n}(OH)_n]^{2-}$ (n = 1−5) complexes, with the consequence that no isotopomer-based $^{35/37}Cl$-resolved isotope effects are visible for the hydroxido complexes, in contrast to that observed in the aquated $[PtCl_{6-n}(H_2O)_n]^{(2-n)-}$ (n = 1−5) series of complexes.[29,30] However, the exquisite additional *isotopomer*-based intrinsic $^{1}\Delta^{195}Pt(^{18/16}O)$ isotope effects visible in the ^{195}Pt NMR profiles of the $[Pt^{35/37}Cl_{6-n}(^{16/18}OH)_n]^{2-}$ complex anions upon partial ^{18}O enrichment (ca. 45%) of the $Na^{18}OH$ experimentally confirm this interpretation and highlight the importance of the trans influence of the ligands in the intrinsic $^{1}\Delta^{195}Pt(^{37/35}Cl)$ and $^{1}\Delta^{195}Pt(^{18/16}O)$ isotope effects in the ^{195}Pt NMR spectra of the platinum(IV) complexes such as presented in this paper.

DOI: 10.1021/ic502901d
Inorg. Chem. 2015, 54, 2752−2764

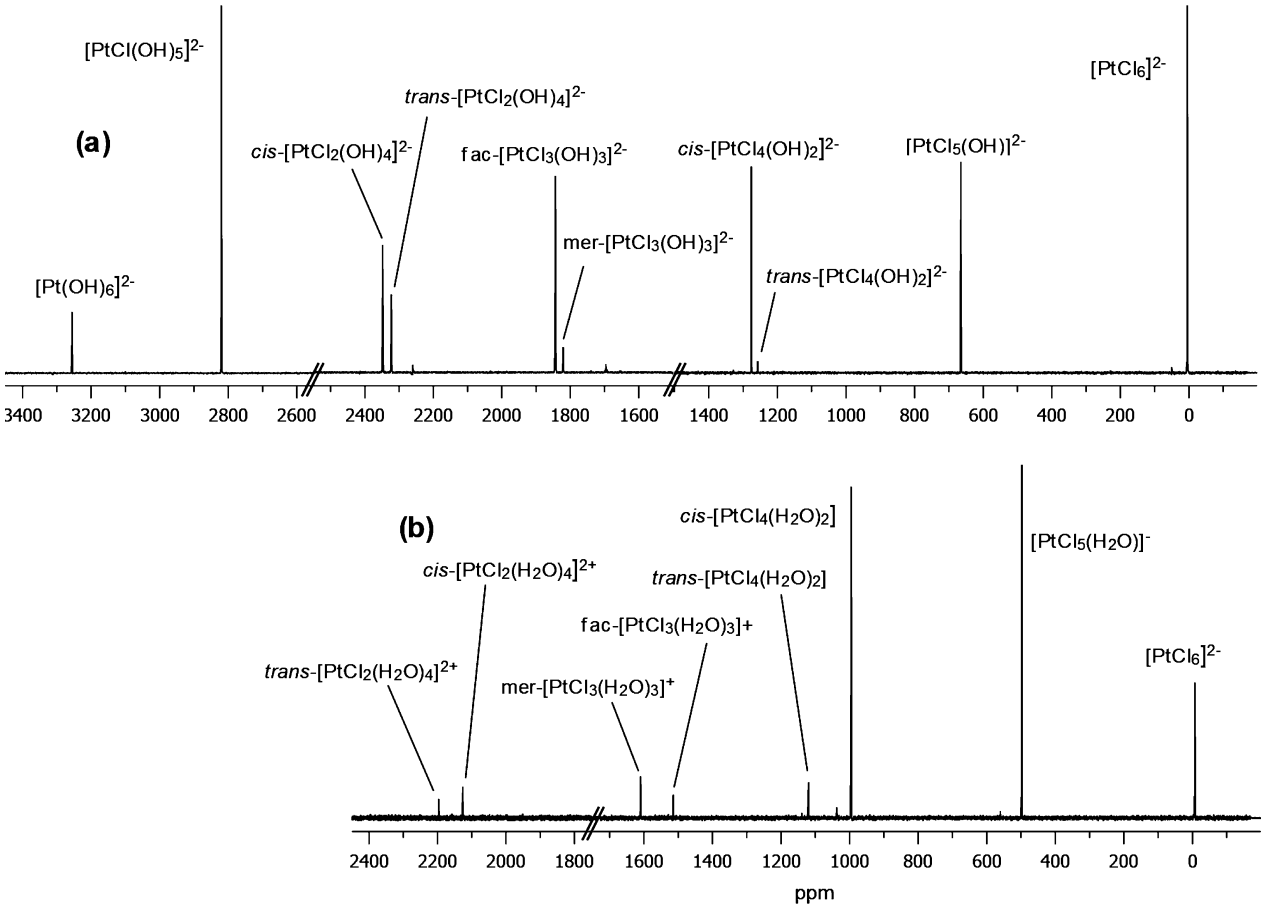

Figure 1. ^{195}Pt NMR spectra (ca. 129 MHz) of (a) 0.4 M Na_2PtCl_6 dissolved in an aqueous 4 M NaOH solution, recorded over the course of several days, showing signals of the complexes $[PtCl_{6-n}(OH)_n]^{2-}$ (n = 0–6) and (b) 0.2 M K_2PtCl_4 in 1 M $HClO_4$ aged for ca. 12 h, followed by oxidation with 5 equiv of $NaClO_3$ showing signals of $[PtCl_{6-n}(H_2O)_n]^{(2-n)-}$ (n = 0–4). All spectra were recorded at 293 K.

EXPERIMENTAL SECTION

Reagents and Sample Preparation. Reagents were obtained from commercial sources and were used without further purification. $Na_2[PtCl_6]\cdot 6H_2O$ (Johnson Matthey PLC, Precious Metals Division) was of reagent grade (99%) and was dried in vacuo at 333 K and stored in a desiccator prior to use. NMR samples were prepared by dissolving $Na_2[PtCl_6]\cdot 6H_2O$ (to a final platinum concentration of 0.4 M) in a 1–2 mL strongly alkaline aqueous solution of 4.0 M NaOH (Aldrich) in ultrapure Milli-Q water (electrical resistance greater than 18 MΩ), which typically contained 50% D_2O (99.9 atom % D, Sigma-Aldrich) by volume for NMR magnetic field locking purposes. Samples with ^{18}O enrichment were prepared by dissolving an appropriate mass of $Na_2[PtCl_6]\cdot 6H_2O$ in an alkaline solution (4.0 M NaOH) consisting of a 55:45 mixture by volume of D_2O and $H_2{}^{18}O$ (97 atom % ^{18}O, Isotec) and allowed to equilibrate for ca. 24 h at room temperature under conditions of ambient light. The initially bright-orange solutions obtained changed color from golden yellow to a pale light yellow over the course of ca. 24 h at room temperature. In order to assess the possibility of dissolved oxygen leading to slightly broader ^{195}Pt NMR line widths, samples were initially degassed by freeze–pump–thaw cycles under nitrogen, although this procedure was found to be unnecessary, having little effect on the achievable ^{195}Pt NMR resolution or line width. While detailed studies of the reaction kinetics were beyond the scope of the current study, the results of a time-arrayed ^{195}Pt NMR experiment, shown in the Supporting Information (SI; Figure S1), give a semiqualitative view of the changes in the chemical species distribution as a function of time in these solutions, showing that an apparent equilibrium distribution of four species is only achieved after >50 h at 293 K, in the absence of visible light. Because the NMR spectra were recorded under dynamic conditions, it follows that no information regarding the equilibrium concentrations or accurate information about the relative thermodynamic stabilities of the series of $[PtCl_{6-n}(OH)_n]^{2-}$ (n = 0–6) anions should be inferred from ^{195}Pt NMR signal intensity data in these spectra because, during a typical ^{195}Pt NMR acquisition time, the intensities of the peaks may change in solutions not at steady state.

^{195}Pt NMR Spectroscopy. ^{195}Pt NMR spectra were recorded at 293 K using a Varian INOVA 600 (B_0 = 14.1 T), operating at 128.8 MHz for ^{195}Pt, equipped with a 5 mm broad-band probe (internal ^{2}H magnetic field locking was employed throughout). Probe temperatures were calibrated using the standard methanol/ethylene glycol ^{1}H chemical shift technique; probe temperatures were controlled using the standard variable-temperature unit of the instrument (temperature regulation estimated at ±0.1 K). After insertion of samples into the NMR probe, they were allowed to reach thermal equilibrium for at least 15 min before data acquisition was started. ^{195}Pt NMR chemical shifts were referenced to the signal of $[PtCl_6]^{2-}$ (δ = 0 ppm) in an external reference solution [500 mg/mL $H_2[PtCl_6]\cdot 6H_2O$ in 30% (v/v) D_2O/1 M HCl] at 293 K. NMR spectra were recorded using a spectral width of 200 kHz and a 60° pulse-width data acquisition time of between 0.5 and 1.0 s with a preacquisition delay of 1.0 s; ^{195}Pt T_1 relaxation times were measured for some of these complexes using the inversion–recovery sequence, showing these to be <1 s at 293 K. In order to achieve a satisfactory signal-to-noise level for least-squares fitting of functions describing isotope effects, it was typically necessary to collect some 20000 transients. All spectra were processed using the *MestReNova 7.1.1* software,[34] with raw free induction decay data being zero-filled to achieve adequate digital resolution, with no apodization functions being applied, so that the intrinsic $^1\Delta^{195}Pt(^{37/35}Cl)$ and $^1\Delta^{195}Pt(^{18/16}O)$ isotope shifts of the ^{195}Pt NMR profile could be deconvoluted at natural line width as accurately as possible.

DOI: 10.1021/ic502901d
Inorg. Chem. 2015, 54, 2752–2764

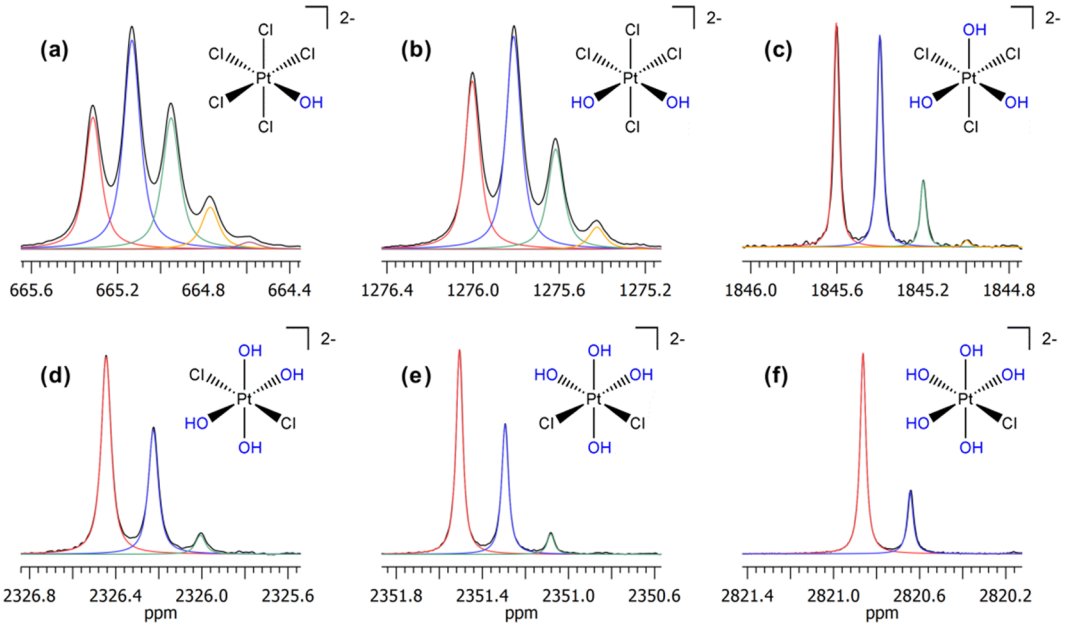

Figure 2. Expanded 128.8 MHz ^{195}Pt NMR intrinsic $^{1}\Delta^{195}$Pt($^{37/35}$Cl) profiles of (a) $[Pt^{35/37}Cl_5(OH)]^{2-}$, (b) *cis*-$[Pt^{35/37}Cl_4(OH)_2]^{2-}$, (c) *fac*-$[Pt^{35/37}Cl_3(OH)_3]^{2-}$, (d) *trans*-$[Pt^{35/37}Cl_2(OH)_4]^{2-}$, (e) *cis*-$[Pt^{35/37}Cl_2(OH)_4]^{2-}$, and (f) $[Pt^{35/37}Cl(OH)_5]^{2-}$ in aqueous solution at 293 K (black lines) and results of signal deconvolution procedures (colored lines; see the text for details).

Deconvolution of the experimental ^{195}Pt NMR profiles was performed using the line-fitting feature implemented in *MestReNova 7.1.1* (least-squares algorithm), modeling the experimental profile as the sum of a set of approximate Lorentzian peaks and resulting in excellent agreement between the experimental and deconvoluted spectra.

RESULTS AND DISCUSSION

Generation of $[PtCl_{6-n}(OH)_n]^{2-}$ (n = 0−5) Species and Their $^{1}\Delta^{195}$Pt($^{37/35}$Cl) Isotope Shifts at Natural Abundance. The series of $[PtCl_{6-n}(OH)_n]^{2-}$ (n = 0−5) complexes for ^{195}Pt NMR can be conveniently generated by dissolution of $Na_2[PtCl_6]\cdot 6H_2O$ in a freshly prepared 4 M NaOH solution at 293 ± 0.1 K, as described in the Experimental Section. The resulting slow color change of such solutions from deep orange to bright yellow over a period of many hours indicates a very slow successive replacement of chlorido by hydroxido ligands in these complexes, consistent with previous observations.[32] Simultaneous recording of a series of 128.8 MHz ^{195}Pt NMR spectra with large spectral widths (200 kHz) allows for the semiquantitative distribution of species as a function of time to be constructed, as illustrated in Figure S1 in the SI. Virtually all of the members of the series $[PtCl_{6-n}(OH)_n]^{2-}$ (n = 0−6) are formed during this time, some of which, however, show a transient existence in these highly alkaline solutions. The distribution of species reaches steady state after only 2 days, while four ^{195}Pt NMR signals of the $[PtCl(OH)_5]^{2-}$, *cis*-$[PtCl_2(OH)_4]^{2-}$, *trans*-$[PtCl_2(OH)_4]^{2-}$, and *fac*-$[PtCl_3(OH)_3]^{2-}$ species remain visible in the spectrum after 65 h (Figure S1 in the SI). The hexahydroxido complex $[Pt(OH)_6]^{2-}$ forms extremely slowly under these conditions, with the resonance at $\delta(^{195}Pt) \sim 3256 \pm 2$ ppm ascribed to this complex being observed only after the sample was allowed to stand for several days at room temperature. A representative composite 1D ^{195}Pt NMR spectrum was constructed from three separately recorded ^{195}Pt NMR spectra covering different spectral regions recorded at increasing time intervals for periods of several hours at 293 K, as shown in Figure 1a. This ^{195}Pt NMR spectrum shows the signals of all 10 possible complexes that evolve over time, including the various stereoisomers of the set $[PtCl_{6-n}(OH)_n]^{2-}$ (n = 0−6), with the majority of these complexes being detected within the first hours after dissolution of solid $Na_2[PtCl_6]\cdot 6H_2O$ in aqueous 4 M NaOH containing 50% D_2O. It is interesting to note that the $[PtCl(OH)_5]^{2-}$ and *cis*-$[PtCl_2(OH)_4]^{2-}$ species dominate the spectrum soon after data acquisition and the disappearance of the last trace of the $[PtCl_6]^{2-}$ complex from solution, while other species show only a transient existence as a function of time (see Figure S1 in the SI).

For comparison, Figure 1b shows a ^{195}Pt spectrum (recorded at 293 K) of the corresponding *aquated* complexes $[PtCl_{6-n}(H_2O)_n]^{(2-n)-}$($n$ = 0−4) prepared by the in situ oxidation of 0.2 M $[PtCl_4]^{2-}$ with $NaClO_3$ at 333 K in an aqueous 1 M $HClO_4$ solution.[30] It is worth noting the small but important differences in the experimental $\delta(^{195}Pt)$ chemical shifts between $[PtCl_{6-n}(OH)_n]^{2-}$ (n = 0−5) and their closely related protonated counterparts (Figure 1a,b), which highlight the possibility of ambiguous ^{195}Pt NMR assignments when only of chemical shift $\delta(^{195}Pt)$ data is relied on. By way of illustration, these ^{195}Pt spectra show that the relative order of shielding $[\delta(^{195}Pt)/ppm]$ of the corresponding three sets of possible stereoisomer pairs, *cis*/*trans*-$[PtCl_4(OH)_2]^{2-}$, *fac*/*mer*-$[PtCl_3(OH)_3]^{2-}$, and *cis*/*trans*-$[PtCl_2(OH)_4]^{2-}$, is reversed compared to those of the aquated $[PtCl_{6-n}(H_2O)_n]^{(2-n)-}$ (n = 0−4) complexes. The *trans*-$[PtCl_4(OH)_2]^{2-}$ species $[\delta(^{195}Pt) \sim 1257$ ppm], for example, is more shielded by ∼19 ppm compared to its cis stereoisomer $[\delta(^{195}Pt) \sim 1276$ ppm], while the aquated *cis*-$[PtCl_4(H_2O)_2]$ stereoisomer $[\delta(^{195}Pt) \sim 996$ ppm] is relatively more shielded by 134 ppm relative to its trans isomer $[\delta(^{195}Pt) \sim 1134$ ppm]. Moreover, the extent of $\delta(^{195}Pt)$ chemical shift differences between the aquated complexes decreases for each isomer pair in the order *cis*/*trans*-$[PtCl_4(H_2O)_2]$ (∼100 ppm) > *fac*/*mer*-$[PtCl_3(H_2O)_3]^{+}$ (∼60 ppm) > *cis*/*trans*-$[PtCl_2(H_2O)_4]^{2+}$ (∼40 ppm), while the reverse trend is found for the corresponding hydroxido

DOI: 10.1021/ic502901d
Inorg. Chem. 2015, 54, 2752−2764

complex isomer pairs. Such subtle differences in chemical shift trends highlight the high sensitivity of ^{195}Pt NMR shielding to structural differences and other extraneous effects (e.g., solution temperature and concentration and even the pH in aqueous solution) for these compounds. This makes unambiguous assignments of ^{195}Pt NMR resonances of such platinum(IV) complexes in less well-defined solutions (e.g., industrial process feed streams or catalyst precursor solutions), based on *only* experimental chemical shifts $\delta(^{195}\mathrm{Pt})$/ppm, tedious and potentially subject to inaccuracies. Thus, the unique isotopic profiles of the ^{195}Pt NMR peaks serve as an unambiguous confirmation of the correct assignments of these platinum complexes, which is a considerable advantage in this context.

The expanded ^{195}Pt NMR resonance profiles of six of the predominantly observed $[PtCl_{6-n}(OH)_n]^{2-}$ (n = 0−5) anions in Figure 1a, recorded under carefully optimized NMR acquisition conditions and temperature control at 293 ± 0.1 K, show that their individual ^{195}Pt resonances are not single peaks but that each is resolved into a characteristic fine structure, as a consequence of *intrinsic* $^{35/37}$Cl isotope effects. The set of the expanded ^{195}Pt NMR resonances for each of the complex anions (a) $[Pt^{35/37}Cl_5(OH)]^{2-}$, (b) *cis*-$[Pt^{35/37}Cl_4(OH)_2]^{2-}$, (c) *fac*-$[Pt^{35/37}Cl_3(OH)_3]^{2-}$, (d) *cis*-$[Pt^{35/37}Cl_2(OH)_4]^{2-}$, (e) *trans*-$[Pt^{35/37}Cl_2(OH)_4]^{2-}$, and (f) $[Pt^{35/37}Cl(OH)_5]^{2-}$ is displayed in Figure 2, illustrating the well-resolved unique intrinsic isotope ^{195}Pt NMR profile of each species.

The intrinsic $^1\Delta^{195}Pt(^{37/35}Cl)$ isotope ^{195}Pt NMR resonance profiles of each species in Figure 2 can be deconvoluted into a sum of Lorentzian peaks (colored lines), fitted to the experimental NMR spectrum by least squares using the algorithm implemented in the commercial *MestReNova 7.1.1* software.[34] It is worth noting that the resultant ^{195}Pt NMR peak profiles of the these $[PtCl_{6-n}(OH)_n]^{2-}$ complexes are clearly resolved into only isotopologue-based fine structures ranging from six to two individual Lorentzian peaks for this series of complex anions. At natural abundance of $^{35/37}$Cl and ^{16}O, the ^{195}Pt NMR profile is consistent only with the intrinsic $^1\Delta^{195}Pt(^{37/35}Cl)$ isotope shifts corresponding to all statistically possible $^{35/37}$Cl isotopologues of each hydroxidochloridoplatinum(IV) anion, conforming to a simple "rule" giving $(6 - n) + 1$ resolved isotopologue peaks for n bound hydroxido ligands in this series of complex anions. The natural abundance (ρ) of a given isotopologue of a given complex anion is readily calculated from multinomial probability theory, using the fractional abundances of the isotopes (ρ_i) according to equation

$$\rho(n_1, n_2, ..., n_x) = \frac{(\sum_{i=1}^{x} n_i)!}{\prod_{i=1}^{x} (n_i!)}\left[\prod_{i=1}^{x} (\rho_i)^{n_i}\right] \quad (1)$$

where n_x is the number of a given isotope x in the isotopologue at natural abundance ρ_x.[29,30] On the basis of the natural abundances of chlorine isotopes (ρ^{35}_{Cl} = 0.7553 and ρ^{37}_{Cl} = 0.2447),[35] the calculated relative statistical abundances of each set of isotopologues of every anion of this series are in excellent agreement with the relative peak areas determined by deconvolution of their ^{195}Pt NMR signals obtained at 293 ± 0.1 K, as shown in Table 1.

Remarkably, the intrinsic $^1\Delta^{195}Pt(^{37/35}Cl)$ isotope effects visible in the ^{195}Pt NMR peak profile of selected members of the corresponding protonated $[PtCl_{6-n}(H_2O)_n]^{(2-n)-}$ (n = 1−4) complexes show additional *isotopomer*-resolved fine structure,[29,30] as illustrated in the interest of clarity in Figure 3. Comparison of the ^{195}Pt NMR peak profile of $[PtCl_5(H_2O)]^-$ with that of the $[PtCl_5(OH)]^{2-}$ species is fascinating. The profile of the latter is clearly resolved into a six-line pattern [$(6 - n) + 1$ for n = 1] corresponding to all possible $^{35/37}$Cl isotopologues (Figure 3a), while that of the $[PtCl_5(H_2O)]^-$ anion shows the additional isotopomer-resolved fine structure (Figure 3b indicated by peaks 1 and 2), as was demonstrated previously.[29] The additional fine structure of the ^{195}Pt NMR profile of the $[PtCl_5(H_2O)]^-$ anion is due to the fact that for the isotopologue $[Pt^{35}Cl_4{}^{37}Cl(H_2O)]^-$, for example, only one *isotopomer* in which a ^{37}Cl ion is coordinated trans to a H_2O molecule is possible, compared to four isotopomers (present statistically in a 4:1 ratio) in which a ^{35}Cl is trans to the bound water molecule.[29,30] Consequently, the slightly more shielded trans ^{37}Cl−Pt−OH_2 isotopomer is recognizable by the small shoulder in the ^{195}Pt NMR profile for the $[Pt^{35}Cl_4{}^{37}Cl(H_2O)]^-$ isotopologue, as illustrated by the fitted color-coded Lorentzian peaks for this (and other isotopologues) in Figure 3b. While similar isotopomers are obviously possible for the $[PtCl_5(OH)]^{2-}$ anion (i.e., ^{35}Cl or ^{37}Cl trans to a hydroxido ligand), evidently these are not resolved in the ^{195}Pt NMR profile of the hydroxido complex. We argue in this paper that such striking differences between the ^{195}Pt NMR peak profiles of the $[PtCl_{6-n}(OH)_n]^{2-}$ (n = 1−5) anions compared to the $[PtCl_{6-n}(H_2O)_n]^{(2-n)-}$ (n = 1−5) series of complexes are most likely a consequence of the relatively higher trans influence of the OH^- ligand,[33] which when coordinated trans to either a ^{35}Cl or ^{37}Cl isotope chlorido ion, results in the vibrationally averaged effective Pt−$^{35/37}$Cl bond displacement being just too long for isotopomer effects to be resolved in the ^{195}Pt NMR peak profile of the isotopologue of the $[PtCl_5(OH)]^{2-}$ anions. This idea is consistent with the work of Gombler,[21] who found that the $^1\Delta^{77}Se(^{13/12}C)$ isotope shift in a series of closely related methyl- and trifluoromethyl-substituted selenium compounds in solution is inversely proportional to the mean Se−C bond length.

Table 1. Comparison between the Experimental Intrinsic $^1\Delta^{195}Pt(^{37/35}Cl)$ Isotope Profiles Obtained by Signal Deconvolution (Line Fitting) and the Statistically Possible $^{35/37}$Cl Isotopologues Calculated at Natural Abundance for the Complexes $[Pt^{35/37}Cl_5(^{16}OH)]^{2-}$ and *cis*-$[Pt^{35/37}Cl_4(^{16}OH)_2]^{2-}$ in Aqueous Solution (Figure 2) at 293 K, Showing Excellent Agreement (Additional Data Are Shown in the SI, Table S1)

		.natural abundance/%	
isotopic formula[a]	isotope shift[b]/ppm	experimental[c]	calculated
$[Pt^{35}Cl_5(^{16}OH)]^{2-}$	0	24.58	24.97
$[Pt^{35}Cl_4{}^{37}Cl(^{16}OH)]^{2-}$	−0.182	39.64	39.93
$[Pt^{35}Cl_3{}^{37}Cl_2(^{16}OH)]^{2-}$	−0.364	25.79	25.54
$[Pt^{35}Cl_2{}^{37}Cl_3(^{16}OH)]^{2-}$	−0.545	8.35	8.17
$[Pt^{35}Cl^{37}Cl_4(^{16}OH)]^{2-}$	−0.727	1.65	1.31
$[Pt^{37}Cl_5(^{16}OH)]^{2-}$	*d*	*d*	0.08
cis-$[Pt^{35}Cl_4(^{16}OH)_2]^{2-}$	0	32.68	32.96
cis-$[Pt^{35}Cl_3{}^{37}Cl(^{16}OH)_2]^{2-}$	−0.193	41.92	42.16
cis-$[Pt^{35}Cl_2{}^{37}Cl_2(^{16}OH)_2]^{2-}$	−0.385	20.36	20.22
cis-$[Pt^{35}Cl^{37}Cl_3(^{16}OH)_2]^{2-}$	−0.577	4.60	4.32
cis-$[Pt^{37}Cl_4(^{16}OH)_2]^{2-}$	−0.774	0.44	0.34

[a] ^{195}Pt. [b] Relative to the lightest isotopologue in the set. [c] From fitted peak areas. [d] Not reliably measured.

DOI: 10.1021/ic502901d
Inorg. Chem. 2015, 54, 2752−2764

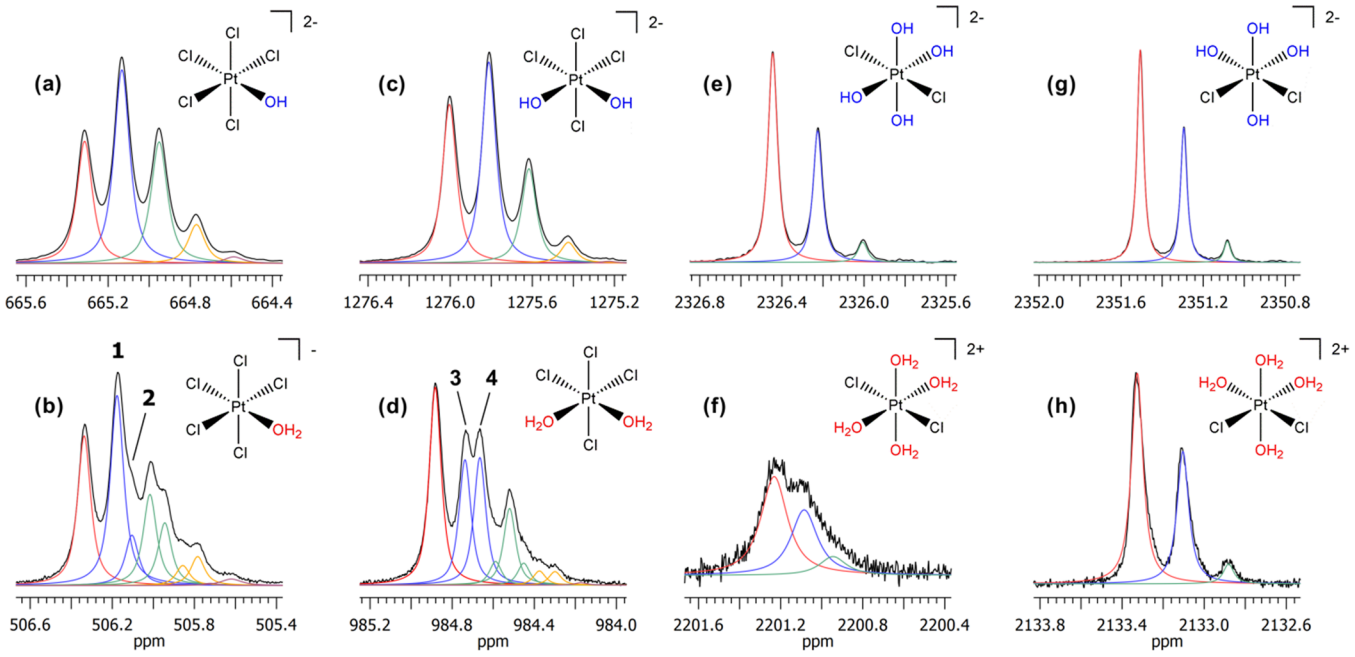

Figure 3. Comparison of the 128.8 MHz ^{195}Pt NMR $^{1}\Delta^{195}$Pt($^{37/35}$Cl) profiles of selected chloridohydroxidoplatinum(IV) complexes to their corresponding aquated counterparts at natural abundance ^{16}O: (a) $[PtCl_5(OH)]^{2-}$, (b) $[Pt^{35/37}Cl_5(H_2O)]^{-}$, (c) *cis*-$[Pt^{35/37}Cl_4(OH)_2]^{2-}$, (d) *cis*-$[Pt^{35/37}Cl_4(H_2O)_2]$, (e) *trans*-$[Pt^{35/37}Cl_2(OH)_4]^{2-}$, (f) *trans*-$[Pt^{35/37}Cl_2(H_2O)_4]^{2+}$, (g) *cis*-$[Pt^{35/37}Cl_2(OH)_4]^{2-}$, and (h) *cis*-$[PtCl_2(H_2O)_4]^{2+}$. Assignments of peaks 1−4 discussed in the text.

The differences between the ^{195}Pt NMR peak profiles observed for the geometrically identical *cis*-$[Pt^{35/37}Cl_4(OH)_2]^{2-}$ and its corresponding uncharged *cis*-$[Pt^{35/37}Cl_4(H_2O)_2]$ complex are even more pronounced (Figure 3c,d). The ^{195}Pt NMR peak of the former species is resolved into only a five-line $[(6 - n) + 1$ for $n = 2)$ isotopologue pattern, while the ^{195}Pt NMR profile of the corresponding aquated *cis*-$[Pt^{35/37}Cl_4(H_2O)_2]$ complex clearly shows additional "fine structure" as a consequence of two nonequivalent isotopomers that are possible in the *cis*-$[Pt^{35}Cl_3{}^{37}Cl(H_2O)_2]$ isotopologue.[30] The two isotopomers responsible for the additional $^{1}\Delta^{195}$Pt($^{37/35}$Cl) isotope "splitting" of the *cis*-$[Pt^{35}Cl_3{}^{37}Cl(H_2O)_2]$ isotopologue are reflected by two equally intense partially resolved experimental peaks (3 and 4) in Figure 3d. These result from two isotopomer configurations that occur with statistically equal probabilities of 21.08%,[29,30] corresponding to one in which ^{37}Cl and ^{35}Cl ions are coordinated trans to the two water molecules and one in which two ^{35}Cl ions are trans to the water molecules in the *cis*-$[Pt^{35}Cl_3{}^{37}Cl(H_2O)_2]$ isotopologue. The additional fine structure of the remaining isotopologues of *cis*-$[Pt^{35}Cl_2{}^{37}Cl_2(H_2O)_2]$, *cis*-$[Pt^{35}Cl^{37}Cl_3(H_2O)_2]$, and *cis*-$[Pt^{37}Cl_4(H_2O)_2]$ similarly accounts for the fine structure of the ^{195}Pt NMR peak profile in Figure 3d.[30] Clearly, such an additional fine structure due to $^{35/37}$Cl isotopomers in the ^{195}Pt NMR profile (Figure 3c) in the corresponding *cis*-$[Pt^{35/37}Cl_4(OH)_2]^{2-}$ anion is *not* observed, most probably because of the high trans influence of OH^-, resulting in the Pt−Cl bond lengths trans to OH^- in the *cis*-$[Pt^{35/37}Cl_4(OH)_2]^{2-}$ anion being presumably just too long to be resolved in the ^{195}Pt NMR profiles recorded under these conditions.

The ^{195}Pt NMR profiles of the pair of *trans*/*cis*-$[PtCl_2(OH)_4]^{2-}$ complexes (Figure 3e,g) closely resemble one another, both showing only three $[(6 - n) + 1$ for $n = 4]$ isotopologue peaks, spaced by a $^{1}\Delta^{195}$Pt($^{37/35}$Cl) isotope shift of ∼−0.22(3) ppm, apart from only slightly broader NMR line widths ($\nu_{1/2}$ ∼ 7 Hz vs 5 Hz) of the *trans*-$[PtCl_2(OH)_4]^{2-}$ (Figure 3e) compared to the *cis*-$[PtCl_2(OH)_4]^{2-}$ isotopologue peaks at 293 K (Figure 3g). In the *trans*-$[PtCl_2(OH)_4]^{2-}$ complex, because the chlorido ions are mutually trans to each other, no $^{35/37}$Cl trans to the hydroxido ligands are possible, resulting in only isotopologue resolution visible in the ^{195}Pt NMR profiles, corresponding to the *trans*-$[Pt^{35}Cl_2(OH)_4]^{2-}$, *trans*-$[Pt^{35}Cl^{37}Cl(OH)_4]^{2-}$, and *trans*-$[Pt^{37}Cl_2(OH)_4]^{2-}$ species, respectively. In the *cis*-$[Pt^{35/37}Cl_2(OH)_4]^{2-}$ complex, for any of the possible isotopologues of this anion, no $^{35/37}$Cl isotopomers are resolved because of the high trans influence of the OH^- ligand because the Pt−$^{35/37}$Cl bonds are presumably just too long for isotopomer-based resolution to be observed, thus resulting in a very similar experimental three-line profile at this magnetic field strength. Comparison of the ^{195}Pt NMR profiles of the *trans*/*cis*-$[PtCl_2(OH)_4]^{2-}$ anions (Figure 3e,g) to those of the corresponding aquated *cis*- and *trans*-$[Pt^{35/37}Cl_2(H_2O)_4]^{2+}$ cations (Figure 3f,h) is interesting because the strikingly similar $^{35/37}$Cl isotopologue profiles of *trans*/*cis*-$[PtCl_2(OH)_4]^{2-}$ species differ from the corresponding aquated counterparts. The *trans*-$[Pt^{35/37}Cl_2(H_2O)_4]^{2+}$ cation shows a poorly resolved three-line ^{195}Pt NMR profile, with a small intrinsic $^{1}\Delta^{195}$Pt($^{37/35}$Cl) ∼ 0.14(4) ppm isotope shift and significantly broader line widths ($\nu_{1/2}$ ∼ 20 Hz; Figure 3f) resolved only at the isotopologue level; on the other hand, the *cis*-$[Pt^{35/37}Cl_2(H_2O)_4]^{2+}$ isomer shows a well-spaced three-line ^{195}Pt NMR profile, very similar to those for the corresponding hydroxido anions (Figure 3h), although with somewhat broader line widths.[30] Nevertheless, in all of the dichloridotetrahydroxido or dichloridotetraaqua complexes, no $^{35/37}$Cl isotopomer effects are possible for their isotopologues for natural abundance ^{16}O. However, as will be seen below, isotopomer-resolved effects *are* visible on ^{18}O enrichment in the pair of *trans*/*cis*-$[PtCl_2(OH)_4]^{2-}$ anions. The latter effects result in unique ^{195}Pt NMR isotope profiles, enabling the unambiguous

DOI: 10.1021/ic502901d
Inorg. Chem. 2015, 54, 2752−2764

^{195}Pt NMR assignment of the pair of *trans*/*cis*-$[PtCl_2(OH)_4]^{2-}$ anions, as we have shown also for their corresponding aquated *cis*/*trans*-$[Pt^{35/37}Cl_2(H_2O)_4]^{2+}$ cations previously.[30]

For completeness, it should be mentioned here that isotope effects due to $^{35/37}$Cl and $^{16/18}OH_2$ for selected chloridoaqua complexes of platinum(II) and platinum(IV) have previously been reported by Gröning and Elding,[18] although the resolution of the 103 MHz ^{195}Pt NMR profile was rather poor and only resolution at the isotopologue level was presumed, probably as a result of the use of a lower-field NMR magnet of ∼8.46 T. Moreover, the authors report obtaining inter alia only the *mer*-$[PtCl_3(H_2O)_3]^+$ cation by oxidation of $[PtCl_4]^{2-}$ with excess Cl_2 in perchloric acid. In our solutions, we obtained both the *mer*-$[PtCl_3(H_2O)_3]^+$ and *fac*-$[PtCl_3(H_2O)_3]^+$ species, which are readily distinguished by their unique 128 MHz NMR $^{35/37}$Cl and $^{16/18}$O isotope profiles at carefully controlled temperatures.[29] The *mer*-$[PtCl_3(H_2O)_3]^+$ cation, in fact, shows both isotopologue and isotopomer resolution, while in alkaline solutions, we find too low concentration of the corresponding *mer*-$[PtCl_3(OH)_3]^{2-}$ species for reliable isotope profiling, while the *fac*-$[PtCl_3(OH)_3]^{2-}$ $^{35/37}$Cl isotope profile consists of only a three-line isotopologue profile.

In broad terms, therefore, these interesting, if subtle, differences in the intrinsic $^1\Delta^{195}Pt(^{37/35}Cl)$ isotope effects observed in the $[PtCl_{6-n}(OH)_n]^{2-}$ (n = 1−5) anions, compared to their aquated (protonated) $[PtCl_{6-n}(H_2O)_n]^{(2-n)-}$ (n = 1−5) analogues,[29,30] can be understood in the context of the very high sensitivity of the $\sigma(^{195}Pt)$ nuclear shielding to extremely small differences in Pt−X (X = $^{35/37}$Cl/OH/OH_2) bond displacements in their respective isotopologues (and when possible isotopomers), as previously predicted by the elegant theoretical work of Jameson et al.[36−42] and in subsequent density functional theory (DFT) computational studies.[14,43−46] Generally, the intrinsic isotope shift for an NMR-active nucleus M bound to isotope X in a compound MX can be written as

$$^n\Delta M(^{m'/m}X) = \sigma_M - \sigma_M^* = \delta_M^* \quad (2)$$

after the notation of Gombler[21] and Jameson,[38] where m and m' are the mass numbers of the light and heavy isotopes of element X, respectively, bound to M, with n indicating the number of chemical bonds separating atoms M and X, and σ_M and δ_M represent the magnetic shielding and chemical shift of nucleus M, with the asterisk indicating the quantities pertaining to the heavier isotope. It follows from the above definition that isotope shifts are usually *negative*; i.e., the heavier isotope usually induces greater shielding or negative chemical shift change (after the sign convention proposed by Gombler[21] and Wasylishen et al.[25]). Jameson et al. decades ago demonstrated a theoretical framework toward understanding the effects of isotopic substitution and temperature on the magnetic shielding of NMR-active metal nuclei in octahedral $[MX_6]$ and $[M(XY)_6]$ molecules and metal complexes.[37−42] These studies indicate that the magnitude of an intrinsic isotope effect on the chemical shift observed in the NMR resonance of a metal M must be understood in terms of the anharmonic "rovibrational" averaging of the M−X bond displacements, which, in turn, are a function of the mass factor $(m' - m)/m'$, where m' and m are the masses of the heavy and light isotopes of X.[39−42]

In this light, the experimentally observed differences in the intrinsic $^1\Delta^{195}Pt(^{37/35}Cl)$ isotope-shift-induced profile of the ^{195}Pt NMR peaks of the $[PtCl_{6-n}(OH)_n]^{2-}$ (n = 1−5) anions, compared to their corresponding aquated analogues, may qualitatively be accounted for in terms of very small differences in the effective Pt−OH/H_2O/Cl bond displacements due to differences in the relative trans influence of ligands in these octahedral platinum(IV) complexes in solution. Given that the typical trans influence of the ligands in platinum(II) complexes decreases in the order $OH^- > Cl^- > H_2O$[33] and assuming that this order is approximately valid also for platinum(IV) complexes studied herein, it is reasonable to expect a small but significant increase in the Pt−Cl bond distance trans to X in the fragment X−Pt−Cl, following the order HO−Pt−Cl > Cl−Pt−Cl > H_2O−Pt−Cl. Consequently, for the $[PtCl_{6-n}(OH)_n]^{2-}$ (n = 1−5) series of anions, the extent of increase in Pt−$^{35/37}$Cl bond displacement trans to a coordinated hydroxido ligand is apparently just too large to result in detectable $^{35/37}$Cl *isotopomer*-induced $^1\Delta^{195}Pt(^{37/35}Cl)$ isotope shifts in these complex anions (see below). Qualitative support for the importance of the trans influence and the consequent significance of extremely small changes in the vibrationally averaged Pt−$^{35/37}$Cl bond displacements in determining the differences in the intrinsic $^1\Delta^{195}Pt(^{37/35}Cl)$ isotope shifts observed in the ^{195}Pt NMR profiles here is obtained from experimental Pt−(OH_2) and Pt−OH bond displacements observed in the very few single-crystal X-ray diffraction studies of appropriate complexes in the literature. In the only crystal structure that contains a discrete $[PtCl_5(OH)]^{2-}$ anion, to our knowledge, in the literature,[47] the Pt−Cl bond length trans to a hydroxido ligand in the $[PtCl_5(OH)]^{2-}$ anion is 2.310(3) Å. This is significantly longer (by ∼1.61%) than that trans to a water molecule at 2.273(2) Å in the corresponding $[PtCl_5(H_2O)]^-$ anion in the crystal structure of the $[H_{13}O_6][PtCl_5(H_4O_2)]\cdot 2$(18-crown-6) salt, which clearly supports the above hypothesis.[48] Interestingly, the Pt−OH bond distance at 2.06(1) Å trans to a chlorido ion in $[PtCl_5(OH)]^-$ in the solid state[47] is of length similar to that of corresponding Pt−(H_2O) bond of 2.060(6) Å in the $[PtCl_5(H_2O)]^-$ anion.[48] It should be noted that the Pt−OH bond distance of 2.06(1) Å in the crystal structure containing the discrete $[PtCl_5(OH)]^{2-}$ anion[47] is likely, however, to be somewhat uncertain, given the lack of temperature factors in the original diffraction data, which allow for judging the data quality. Nevertheless, these bond displacements are consistent with the higher trans influence of the hydroxido ligand in the order $OH^- > Cl^- > H_2O$ in this context,[33] accounting for the striking differences between the $^{35/37}$Cl isotope ^{195}Pt NMR profiles of the $[PtCl_5(OH)]^{2-}$ and $[PtCl_5(H_2O)]^-$ anions,[29] as shown in parts a and b of Figure 3, respectively. Given the extremely high sensitivity of the DFT-computed ^{195}Pt shielding to very small changes in the Pt−Cl bond displacements, typically ∼ 18300 ppm/Å in the gas phase for $[PtCl_{6-n}Br_n]^{2-}$ anions,[43] it is reasonable to expect that minute changes in the Pt−Cl bond displacements on the order of femtometers can result in detectable changes in the ^{195}Pt shielding of these complexes.[44] Recent DFT computational studies aimed at understanding the possible origin of the experimental intrinsic isotope effects in the series of $[PtCl_{6-n}(OH)_n]^{2-}$ (n = 1−5) anions indeed show that the calculated Pt−Cl bond displacements trans to a hydroxido ligand are, on average, longer than those in the corresponding Pt−Cl distances trans to a coordinated water molecule in $[PtCl_{6-n}(H_2O)_n]^{(2-n)-}$ (n = 1−5) complexes.[45,46] This may be illustrated for geometry-optimized structures of the pair of complexes *cis*-$[PtCl_4(H_2O)_2]$ and *cis*-$[PtCl_4(OH)_2]^{2-}$. The computed Pt−Cl distance trans to

DOI: 10.1021/ic502901d
Inorg. Chem. 2015, 54, 2752−2764

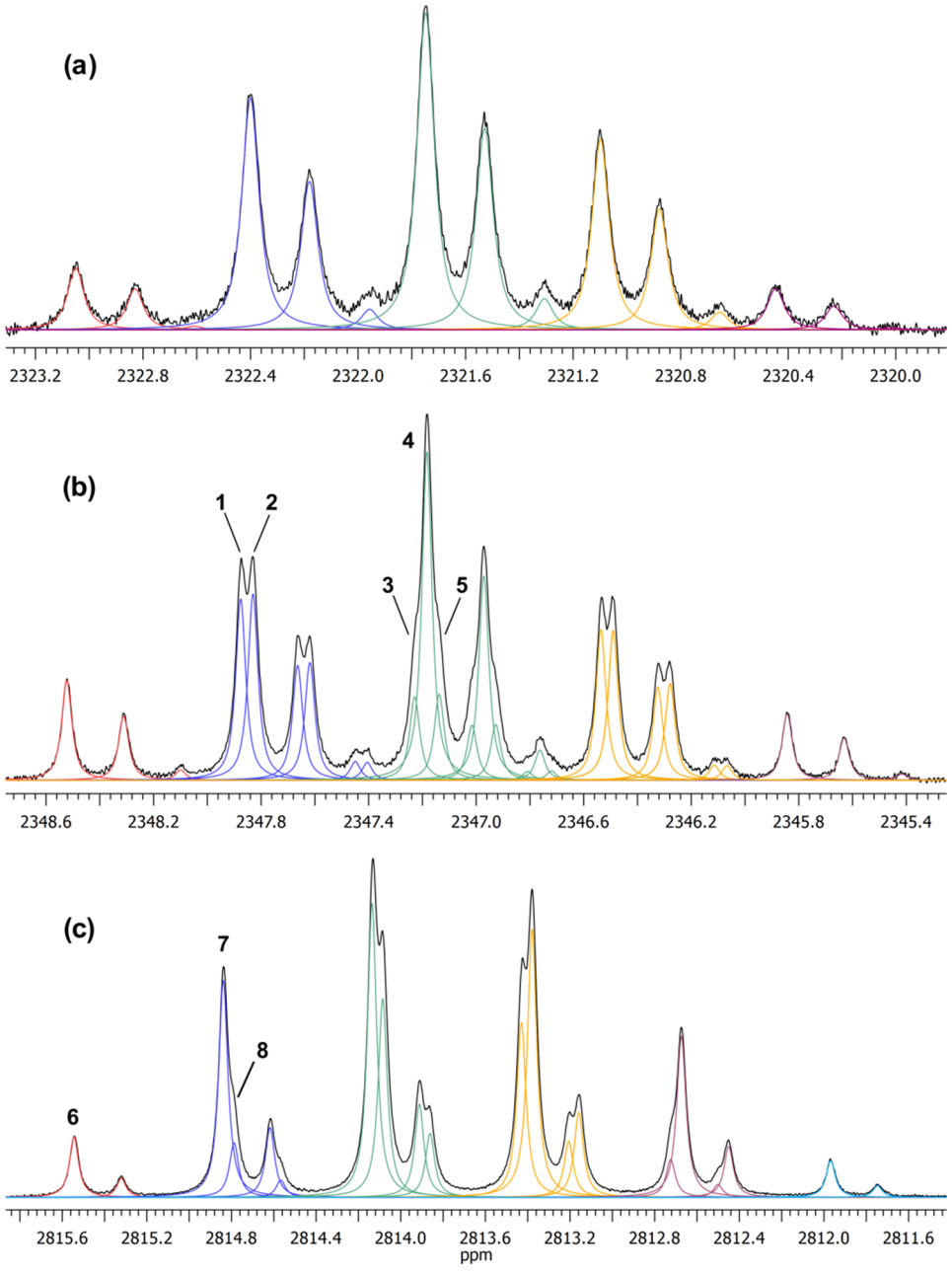

Figure 4. Expanded intrinsic $^{1}\Delta^{195}Pt(^{37/35}Cl)$ and $^{1}\Delta^{195}Pt(^{18/16}O)$ isotope profiles of complexes in an ^{18}O-enriched alkaline aqueous solution (45% ^{18}O-enriched water by volume) at 293 K. (a) *trans*-$[Pt^{35/37}Cl_2(^{16/18}OH)_4]^{2-}$, (b) *cis*-$[Pt^{35/37}Cl_2(^{16/18}OH)_4]^{2-}$, and (c) $[Pt^{35/37}Cl(^{16/18}OH)_5]^{2-}$ resolved at both the isotopologue and isotopomer levels. Assignments of peaks 1−8 are given in Scheme 1 and the text.

a water molecule at 2.2778 Å in the former uncharged *cis*-$[PtCl_4(H_2O)_2]$ species is considerably shorter than the corresponding bond in the *cis*-$[PtCl_4(OH)_2]^{2-}$ anion at 2.4124 Å, while the corresponding Pt−OH_2 and Pt−OH distances are 2.1424 and 2.0107 Å, respectively.[46] For this pair of complexes, the mutually trans Cl−Pt−Cl bond distances in the *cis*-$[PtCl_4(H_2O)_2]$ and *cis*-$[PtCl_4(OH)_2]^{2-}$ species are comparable at 2.3405 and 2.3741 Å, respectively. These theoretical studies clearly support the hypothesis of the importance of the trans influence of a ligand trans to the chlorido ligand in determining the differences in the isotope effects observed for the series of closely related $[PtCl_{6-n}(OH)_n]^{2-}$ (n = 1−5) and $[PtCl_{6-n}(H_2O)_n]^{(2-n)-}$ (n = 1−5) complexes, as shown in this work. Although the DFT-computed zero-point vibrationally averaged ^{195}Pt nuclear shielding trends reasonably reproduce the experimental trends and thus qualitatively support the proposed origin of the intrinsic $^{1}\Delta^{195}Pt(^{37/35}Cl)$ isotope shifts in the ^{195}Pt NMR profiles of the $[PtCl_{6-n}(OH)_n]^{2-}$ (n = 1−5) anions and their $[PtCl_{6-n}(H_2O)_n]^{(2-n)-}$ (n = 1−5) analogues, satisfactory *quantitative* agreement between computed and experimentally observed intrinsic $^{1}\Delta^{195}Pt(^{37/35}Cl)$ isotope shifts has not yet been achieved.[46] This presumably highlights the complexity of such calculations and the necessity of taking into account dynamic vibrational effects in these complexes, as well as the effects of solvation in the accurate computation of ^{195}Pt NMR shieldings. Particularly in aqueous solution, one might reasonably anticipate significant differences in the solute−solvent hydrogen bonding between the charged $[PtCl_{6-n}(OH)_n]^{2-}$ (n = 1−5) anions and their aquated

DOI: 10.1021/ic502901d
Inorg. Chem. 2015, 54, 2752−2764

$[PtCl_{6-n}(H_2O)_n]^{(2-n)-}$ (n = 1−5) analogues, which range from anionic through uncharged to cationic species.[14,28,45,46] These complexes are doubtlessly highly solvated by water molecules, which is expected to affect the vibrationally averaged bond displacements of Pt−Cl and Pt−OH/OH_2 and thus the intrinsic isotope effects on the ^{195}Pt NMR of the isotopologues and isotopomers as reported here.

Experimental $^1\Delta^{195}Pt(^{18/16}O)$ Isotope Shifts in the ^{195}Pt NMR Profile of $[PtCl_{6-n}(OH)_n]^{2-}$ (n = 1−5) Species. To explore further experimentally the interesting intrinsic isotope effects observable in the ^{195}Pt NMR spectra of the $[PtCl_{6-n}(OH)_n]^{2-}$ (n = 1−5) anions, particularly in the context of the implications of a higher trans influence of OH^- compared to Cl^- (or a water molecule) coordinated to Pt^{IV}, we examined the $^1\Delta^{195}Pt(^{18/16}O)$ isotope shifts in suitably ^{18}O-enriched hydroxido complexes. Interestingly, ^{18}O enrichment cannot be directly achieved by treating $[PtCl_{6-n}(OH)_n]^{2-}$ in alkaline solutions by the simple addition of ^{18}O-enriched water because the rate of hydroxido ligand exchange for $[PtCl_{6-n}(OH)_n]^{2-}$ in alkaline solutions is extremely slow. Practically no ^{18}O for ^{16}O exchange takes place in alkaline solutions over a period of several weeks. This necessitates an alternative method of ^{18}O enrichment. Thus, suitably ^{18}OH-enriched hydroxidoplatinum(IV) complexes can readily be generated by dissolution of $Na_2[PtCl_6]\cdot 6H_2O$ in a freshly prepared 4 M NaOH solution with preenriched water containing $H_2{}^{18}O$ (45% by volume), as described in the Experimental Section. By contrast, convenient $H_2{}^{18}O$ water exchange is possible in acidic solutions for the corresponding $[PtCl_{6-n}(H_2O)_n]^{(2-n)-}$ (n = 1−5) analogues by the simple addition of enriched water to these solutions.[30] Evidently, under acidic conditions, water exchange rates are significantly higher than hydroxido exchange rates in $[PtCl_{6-n}(OH)_n]^{2-}$ anions, emphasizing the extreme kinetic inertness of the hydroxidoplatinum(IV) complexes. These findings are consistent with previous estimates of statistically corrected water exchange rate constants (k_{ex}/s^{-1}) with $H_2{}^{18}O$ in mainly platinum(II) complexes in acidic media by Gröning and Elding,[18] using ^{195}Pt NMR more than 2 decades ago. The estimated water exchange rate constants in the uncharged *cis*-$[PtCl_2(H_2O)_2]$ and cationic $[Pt(H_2O)_4]^{2+}$ complex range from 1.8×10^{-2} to 4.8×10^{-4} s^{-1} for these species, respectively. On the other hand, Dunham and Abbot[49] reported water exchange rate constants for *cis*/*trans*-diaquabis(oxalate)platinum(IV) of $k_{ex} \sim (7 \pm 1.2) \times 10^{-6}$ s^{-1} in 1 M $HClO_4$ at 293 K, while for the corresponding $[Pt(HO)_2(Ox)_2]^{2-}$ complex at pH 5, no ligand exchange rate constants could directly be measured over 190 days, indicative of an estimated hydroxido exchange rate constant of approximately 1×10^{-9} s^{-1} or less. Notably, while the above kinetic studies reported ^{18}O-induced isotope shifts in ^{195}Pt NMR spectra of the platinum(II) complexes, no mention of a more detailed analysis of the remarkable intrinsic $^1\Delta^{195}Pt(^{18/16}O)$ isotope shifts as reported for platinum(IV) complexes in this work was made. This may be ascribed to the lower NMR resolution achievable at lower magnetic field instruments used in these studies and is most probably due to the often significantly broader ^{195}Pt NMR resonances obtained for platinum(II) complexes as a result of the CSA relaxation mechanism prevalent in planar platinum(II) complexes, obscuring any intrinsic $^1\Delta^{195}Pt(^{37/35}Cl)$ isotope shifts.[50]

Figure 4 shows remarkably well-resolved, expanded ^{195}Pt NMR profiles of the *cis*-$[Pt^{35/37}Cl_2(^{16/18}OH)_4]^{2-}$, *trans*-$[Pt^{35/37}Cl_2(^{16/18}OH)_4]^{2-}$, and $[Pt^{35/37}Cl(^{16/18}OH)_5]^{2-}$ anions upon partial enrichment with ^{18}OH as described above, recorded at 293 ± 0.1 K under carefully optimized NMR conditions. These truly remarkable ^{195}Pt NMR profiles display unique intrinsic $^1\Delta^{195}Pt(^{37/35}Cl)$ and $^1\Delta^{195}Pt(^{18/16}O)$ isotope shifts specific to each of the selected stereochemically rigid platinum complex anions, essentially constituting an "NMR fingerprint" based on the statistical distribution of the $^{35/37}$Cl and $^{16/18}$O isotopes in each individual chemical species. Similar unique isotope-resolved ^{195}Pt NMR profiles of other members of the $[PtCl_{6-n}(OH)_n]^{2-}$ (n = 1−5) series of complexes (the ^{195}Pt NMR profiles of the $[Pt^{35/37}Cl_5(^{16/18}OH)]^{2-}$, *cis*-$[Pt^{35/37}Cl_4(^{16/18}OH)_2]^{2-}$, *fac*-$[Pt^{35/37}Cl_3(^{16/18}OH)_3]^{2-}$, and $[Pt(^{16/18}OH)_6]^{2-}$ species are shown in the SI, Figure S2 and Table S1). Inspection of these ^{195}Pt NMR profiles of the series of $[Pt^{35/37}Cl_{6-n}(^{16/18}OH)_n]^{2-}$ (n = 1−5) anions confirms, in general, relatively large intrinsic $^1\Delta^{195}Pt(^{18/16}O)$ isotope shifts up to ca. −0.7 ppm, essentially resulting in n "replicates" of each set of $^{35/37}$Cl isotope-induced NMR profiles of each isotopologue of the specific complex anion in question, as shown for selected examples in Figure 3. The systematic substitution of $^{16}OH^-$ by $^{18}OH^-$ in $[Pt^{35/37}Cl_{6-n}(^{16/18}OH)_n]^{2-}$ (n = 1−5) generates an additional set of ^{18}O-induced isotopologue *and* isotopomer peaks for each set of $^{35/37}$Cl isotopologue peaks resolved in the ^{195}Pt NMR profile. The additional $^1\Delta^{195}Pt(^{18/16}O)$ isotope effects result in the ^{195}Pt resonances becoming progressively more shielded with an increasing number (n) of $^{18}OH^-$ substitutions in the $[PtCl_{6-n}(OH)_n]^{2-}$ (n = 1−5) anions.

The ^{195}Pt NMR profile of the *trans*-$[Pt^{35/37}Cl_2(^{16/18}OH)_4]^{2-}$ complex shown in Figure 4a most clearly illustrates these interesting intrinsic $^1\Delta^{195}Pt(^{37/35}Cl)$ and $^1\Delta^{195}Pt(^{18/16}OH)$ isotope shifts, consisting of five (4 + 1) sets of expected three-line $^{35/37}$Cl isotopologue profiles, color-coded for clarity. The five subsets of three $^{35/37}$Cl-resolved ^{195}Pt NMR profiles of this platinum(IV) anion thus correspond to 15 statistically possible, but magnetically nonequivalent, isotopologues in order of increased shielding of *trans*-$[Pt^{35/37}Cl_2(^{16}OH)_4]^{2-}$ (red), *trans*-$[Pt^{35/37}Cl_2(^{16}OH)_3(^{18}OH)]^{2-}$ (blue), *trans*-$[Pt^{35/37}Cl_2(^{16}OH)_2(^{18}OH)_2]^{2-}$ (green), *trans*-$[Pt^{35/37}Cl_2(^{16}OH)(^{18}OH)_3]^{2-}$ (yellow), and *trans*-$[Pt^{35/37}Cl_2(^{18}OH)_4]^{2-}$ (violet). The sum of the set of 15 Lorentzian peaks obtained by deconvolution using an iterative least-squares algorithm shows a nearly perfect fit of the experimental isotope-resolved ^{195}Pt NMR peaks within the realistic signal-to-noise (S/N) ratio obtained in the spectrum. The individually measured peak areas obtained for each of the best-fit Lorentzian bands arising from the intrinsic $^1\Delta^{195}Pt(^{37/35}Cl)$ and $^1\Delta^{195}Pt(^{18/16}O)$ isotope-induced shifts from the experimental spectrum are in excellent agreement with the calculated statistical abundance of all possible isotopologues, as listed in Table 2. Although for the species *trans*-$[Pt^{35/37}Cl_2(^{16}OH)_2(^{18}OH)_2]^{2-}$ two isotopomers are possible, which may be designated as *trans,trans*-$[Pt^{35/37}Cl_2(^{16}OH)_2(^{18}OH)_2]^{2-}$ and *trans,cis*-$[Pt^{35/37}Cl_2(^{16}OH)_2(^{18}OH)_2]^{2-}$, inspection of the experimental spectrum of this species (Figure 4a) shows that such isotopomers are evidently not resolved, presumably because of the very similar ^{195}Pt NMR shieldings for these two isotopomers. The obvious lack of $^{35/37}$Cl isotopomer resolution in the previously reported ^{195}Pt NMR spectra of the $[Pt^{35/37}Cl_6]^{2-}$ anion,[17,29,39] as well potential $^{16/18}OH^-$ isotopomer resolution in the ^{195}Pt NMR spectrum of the $[Pt(^{16/18}OH)_6]^{2-}$ anion reported here (Figure S2d in the SI),

DOI: 10.1021/ic502901d
Inorg. Chem. 2015, 54, 2752−2764

Table 2. Comparison between Experimental Intrinsic $^{1}\Delta^{195}Pt(^{37/35}Cl)$ and $^{1}\Delta^{195}Pt(^{18/16}O)$ Isotope Profiles Obtained by Signal Deconvolution (Line Fitting) and the Statistically Possible $^{35/37}Cl$ and $^{16/18}O$ Isotopologues and Isotopomers of *trans*-$[Pt^{35/37}Cl_2(^{16/18}OH)_4]^{2-}$ and *cis*-$[Pt^{35/37}Cl_2(^{16/18}OH)_4]^{2-}$ in Aqueous Solution at 293 K (Additional Data Are Shown in the SI, Table S1)

isotopic formula[a]	isotope shift[b]/ppm	abundance/% experimental[c]	abundance/% calculated
trans-$[Pt^{35}Cl_2(^{16}OH)_4]^{2-}$	0	4.07	5.18
trans-$[Pt^{35}Cl^{37}Cl(^{16}OH)_4]^{2-}$	−0.221	2.69	3.36
trans-$[Pt^{37}Cl_2(^{16}OH)_4]^{2-}$	−0.440	0.24	0.54
trans-$[Pt^{35}Cl_2(^{16}OH)_3(^{18}OH)]^{2-}$	−0.650	15.95	17.02
trans-$[Pt^{35}Cl^{37}Cl(^{16}OH)_3(^{18}OH)]^{2-}$	−0.870	10.20	11.03
trans-$[Pt^{37}Cl_2(^{16}OH)_3(^{18}OH)]^{2-}$	−1.092	1.41	1.79
trans-$[Pt^{35}Cl_2(^{16}OH)_2(^{18}OH)_2]^{2-}$	−1.301	22.01	20.99
trans-$[Pt^{35}Cl^{37}Cl(^{16}OH)_2(^{18}OH)_2]^{2-}$	−1.521	13.98	13.60
trans-$[Pt^{37}Cl_2(^{16}OH)_2(^{18}OH)_2]^{2-}$	−1.743	2.15	2.20
trans-$[Pt^{35}Cl_2(^{16}OH)(^{18}OH)_3]^{2-}$	−1.951	13.11	11.50
trans-$[Pt^{35}Cl^{37}Cl(^{16}OH)(^{18}OH)_3]^{2-}$	−2.171	8.32	7.45
trans-$[Pt^{37}Cl_2(^{16}OH)(^{18}OH)_3]^{2-}$	−2.394	1.22	1.21
trans-$[Pt^{35}Cl_2(^{18}OH)_4]^{2-}$	−2.603	2.84	2.36
trans-$[Pt^{35}Cl^{37}Cl(^{18}OH)_4]^{2-}$	−2.820	1.63	1.53
trans-$[Pt^{37}Cl_2(^{18}OH)_4]^{2-}$	−3.031	0.17	0.25
cis-$[Pt^{35}Cl_2(^{16}OH)_4]^{2-}$	0	4.40	5.18
cis-$[Pt^{35}Cl^{37}Cl(^{16}OH)_4]^{2-}$	−0.212	2.81	3.36
cis-$[Pt^{37}Cl_2(^{16}OH)_4]^{2-}$	−0.423	0.45	0.54
cis-$[Pt^{35}Cl_2(^{16}OH)_3(^{18}OH)]^{2-}$	−0.647	7.85	8.79
	−0.694	8.06	8.79
cis-$[Pt^{35}Cl^{37}Cl(^{16}OH)_3(^{18}OH)]^{2-}$	−0.858	4.97	5.52
	−0.904	5.10	5.52
cis-$[Pt^{35}Cl^{37}Cl(^{16}OH)_3(^{18}OH)]^{2-}$	−1.073	0.81	0.90
	−1.118	0.77	0.90
cis-$[Pt^{35}Cl_2(^{16}OH)_2(^{18}OH)_2]^{2-}$	−1.293	3.61	3.50
	−1.340	14.22	13.99
	−1.385	3.73	3.50
cis-$[Pt^{35}Cl^{37}Cl(^{16}OH)_2(^{18}OH)_2]^{2-}$	−1.507	2.38	2.27
	−1.551	8.84	9.07
	−1.596	2.42	2.27
cis-$[Pt^{37}Cl_2(^{16}OH)_2(^{18}OH)_2]^{2-}$	−1.714	0.37	0.37
	−1.760	1.30	1.47
	−1.803	0.40	0.37
cis-$[Pt^{35}Cl_2(^{16}OH)(^{18}OH)_3]^{2-}$	−1.987	6.53	5.75
	−2.032	6.48	5.75
cis-$[Pt^{35}Cl^{37}Cl(^{16}OH)(^{18}OH)_3]^{2-}$	−2.198	4.03	3.73
	−2.244	4.18	3.73
cis-$[Pt^{37}Cl_2(^{16}OH)(^{18}OH)_3]^{2-}$	−2.409	0.65	0.61
	−2.455	0.63	0.61
cis-$[Pt^{35}Cl_2(^{18}OH)_4]^{2-}$	−2.679	2.87	2.36
cis-$[Pt^{35}Cl^{37}Cl(^{18}OH)_4]^{2-}$	−2.891	1.86	1.53
cis-$[Pt^{37}Cl_2(^{18}OH)_4]^{2-}$	−3.105	0.27	0.25

corroborates the absence of isotopomer resolution in the ^{195}Pt NMR spectrum of the *trans*-$[Pt^{35/37}Cl_2(^{16/18}OH)_4]^{2-}$ complex. Evidently, when the same simple ligands with differing isotopes ($^{35/37}Cl^-$ or $^{16/18}OH^-$) are coordinated trans to one another in a platinum(IV) complex, such potential isotopomer isotope effects are not resolved at this magnetic field, probably as a result of too small differences in the bond displacements between the Pt−^{35}Cl and Pt−^{37}Cl or Pt−^{16}O and Pt−^{18}O when mutually trans to one another.

By contrast, the fascinating ^{195}Pt NMR profile of the corresponding stereoisomer *cis*-$[Pt^{35/37}Cl_2(^{16/18}OH)_4]^{2-}$ in Figure 4b shows an additional partially resolved fine structure in some of the five sets of $^{16/18}OH$-induced isotopologue resonances, due to the possibility of magnetically nonequivalent *isotopomers* in these specific isotopologues. Thus, the least and most shielded subsets of ^{195}Pt peaks correspond to the *cis*-$[Pt^{35/37}Cl_2(^{16}OH)_4]^{2-}$ (red peaks) and *cis*-$[Pt^{35/37}Cl_2(^{18}OH)_4]^{2-}$ (violet peaks) complexes, respectively, each consisting of the expected three-peak profile $^{35/37}Cl$ isotopologues in which no isotopomers are possible; the ^{195}Pt NMR profile closely resembles that of the corresponding *trans*-$[Pt^{35/37}Cl_2(^{16/18}OH)_4]^{2-}$ anion (Figure 4a), with the only noticeable difference being somewhat broader peaks in the spectrum of the latter ($\nu_{1/2} \sim 7$ Hz compared to 5 Hz for the cis isomer). However, the neighboring "inner" sets of ^{195}Pt NMR signals corresponding to the isotopologues *cis*-$[Pt^{35/37}Cl_2(^{16}OH)_3(^{18}OH)]^{2-}$ (blue) and *cis*-$[Pt^{35/37}Cl_2(^{16}OH)(^{18}OH)_3]^{2-}$ (yellow) are clearly each split into two additional partially resolved signals of equal intensity, illustrated best by the most intense of the two-line profile of this set (peaks 1 and 2 in Figure 4b). This splitting into two partially resolved peaks in the ^{195}Pt NMR profile of each of these isotopologues of the *cis*-$[PtCl_2(OH)_4]^{2-}$ anion clearly arises from an *isotopomer-induced* intrinsic $^{1}\Delta^{195}Pt(^{18/16}O)$ isotope effects, not unlike those observed in some of the ^{195}Pt NMR spectra of ^{18}O-enriched aquated $[PtCl_{6-n}(H_2O)_n]^{(2-n)-}$ (n = 0−5) analogues.[30] Thus, the partially resolved two-line profile (centered at ∼2347.63 ppm, blue) of the *cis*-$[Pt^{35}Cl_2(^{16}OH)_3(^{18}OH)]^{2-}$ set of isotopologues, the most intense pair of peaks (1 and 2) of this set in the three $^{35/37}Cl$-resolved ^{195}Pt NMR profiles, clearly arises from two possible magnetically nonequivalent isotopomers. In one isotopomer, two ^{16}O isotopes are coordinated trans to the ^{35}Cl ligands, while in the other, ^{16}O and ^{18}O isotopes occupy these sites, with an equal statistical probability of 8.79% [taking into account ca. a 45% (v/v) $H_2{}^{18}O$ enrichment]. This is confirmed by the good agreement of equal measured intensities (7.85 and 8.06% within experimental error) of the Lorentzian peaks 1 and 2 obtained, as shown in Table 2. Similar considerations apply to the two related sets of partially resolved peaks corresponding to the *cis*-$[Pt^{35}Cl^{37}Cl(^{16}OH)_3(^{18}OH)]^{2-}$ and *cis*-$[Pt^{37}Cl_2(^{16}OH)_3(^{18}OH)]^{2-}$ isotopologues occurring at lower statistical abundance of 5.52% and 0.90%, respectively. (The approximately 10% relative error between the estimated peak areas with the statistically expected values is ascribed to experimental error due to the lack of a more accurate knowledge of the degree of ^{18}O enrichment and/or non-negligible errors in the deconvolution procedure.) The second most shielded group of the three pairs of ^{195}Pt peaks [centered around $\delta(^{195}Pt) \sim 2346.24$ ppm, yellow] is similarly ascribed to the various possible $^{16/18}OH$-based isotopomers of the *cis*-$[Pt^{35/37}Cl_2(^{16}OH)(^{18}OH)_3]^{2-}$ isotopologues, which occur in statistical abundances of 5.75%, 3.73%, and 0.61%, respectively. We assign the more shielded of the two signals to the isotopomer in which one $^{18}OH^-$ ion is coordinated trans to the chlorido ligands in this particular isotopologue. The more

DOI: 10.1021/ic502901d
Inorg. Chem. 2015, 54, 2752−2764

shielded of each pair of signals results from the isotopomer in which two ^{18}OH ions occupy two sites trans to the chlorido ligands (regardless of their isotopic identity). Last, the central three-line group of peaks of this ^{195}Pt NMR profile (centered at ~2346.9 ppm, green) corresponds to the set of *cis*-$[Pt^{35/37}Cl_2(^{16}OH)_2(^{18}OH)_2]^{2-}$ isotopologues, with each "peak" showing barely resolved fine structure resulting from *three* possible magnetically nonequivalent isotopomers, due to differing combinations of $^{16/18}$O isotopes coordinated trans to $^{35/37}$Cl ions manifested by only slightly different ^{195}Pt shielding for each. The least shielded, most intense set of signals of this group corresponds to three isotopomers of the *cis*-$[Pt^{35}Cl_2(^{16}OH)_2(^{18}OH)_2]^{2-}$ isotopologue; the most intense central signal (peak 4) of this profile arises from the isotopomer with one ^{16}O and one ^{18}O isotopes trans to ^{35}Cl ions, while the two barely resolved, equally intense Lorentzian peaks (peaks 3 and 5) are assigned to isotopomers in which either both ^{16}O or both ^{18}O isotopes are coordinated trans to the chlorido ligands, respectively. The satisfactory agreement between the deconvoluted Lorentzian peak areas with the calculated statistical probabilities of occurrence of these respective isotopomers in Table 2 confirms these assignments. Moreover, these remarkable ^{195}Pt NMR profiles emphasize again the use of such unique isotopic "NMR fingerprints" as an unambiguous means of distinguishing the stereoisomer pairs of *cis*/*trans*-$[PtCl_2(OH)_4]^{2-}$ complex anions in solution, not easily possible by any other techniques to our knowledge.

A detailed consideration of the ^{195}Pt NMR isotope-induced profile in Figure 4c shows this to consist of 20 (partially resolved) nonequivalent magnetic environments of the ^{195}Pt nucleus in these $[Pt^{35/37}Cl(^{16/18}OH)_5]^{2-}$ anions in a 14.1 T magnetic field (quantitative data in Table 2). This profile can readily be understood to result from 5 + 1 sets of $^{16/18}$O-induced isotopologue peaks, each consisting of 1 + 1 $^{35/37}$Cl isotopologue peaks, with four of the six sets of statistically possible $^{16/18}$O-induced isotopologue peaks being further resolved because of the possible isotopomers with respect to whether ^{16}O or ^{18}O is trans to ^{35}Cl or ^{37}Cl at the specific level of ^{18}O enrichment in this platinum(IV) complex. For example, the peaks indicated by peaks 6–8 in this spectrum result from the isotopologues and isotopomers of the complexes indicated in Scheme 1. The isotope-resolved ^{195}Pt NMR profiles of the

Scheme 1

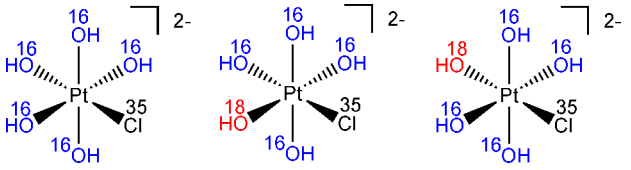

remaining members of the series of $[Pt^{35/37}Cl_{6-n}(OH)_n]^{2-}$ (n = 1–5) anions follow a similar analysis, and these, together with quantitative data, are given in Table S1 in the SI.

Also shown in the SI is the ^{195}Pt NMR spectrum and data of the hexahydroxidoplatinum(IV) anion (Figure S2c in the SI). As may be anticipated, the ^{195}Pt NMR profile of the $[Pt(^{18/16}OH)_6]^{2-}$ anion, centered at $\delta(^{195}Pt)$ ~ 3247.54 ppm, is beautifully resolved into the sharp ^{195}Pt resonances resulting from the statistically expected 6 + 1 $^{16/18}$O isotopologues possible for this complex in aqueous solution at 293 K.

An interesting correlation observed between the experimentally measured $^1\Delta^{195}Pt(^{18/16}O)$ intrinsic isotope shifts and the overall chemical shifts $\delta(^{195}Pt)$/ppm of the $[PtCl_{6-n}(OH)_n]^{2-}$ (n = 1–6) anions is shown in Figure 5. A virtually linear

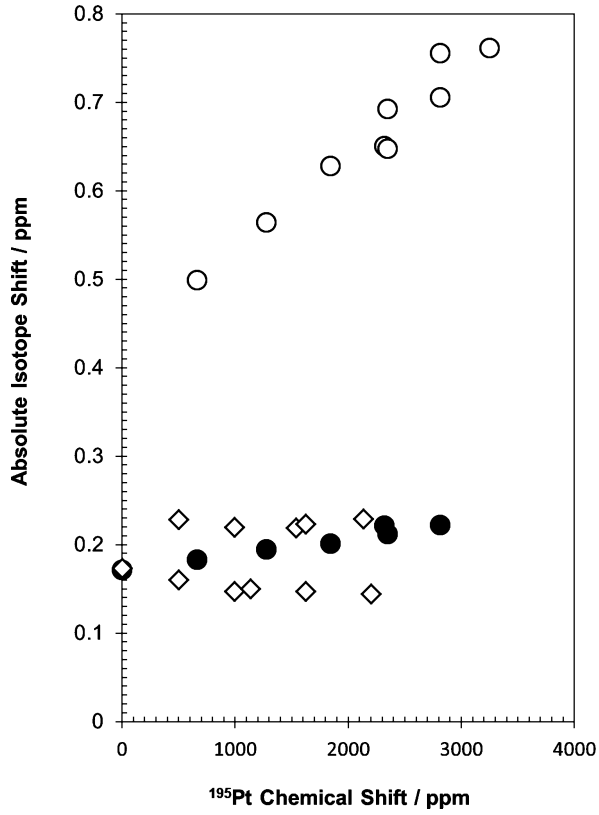

Figure 5. $^1\Delta^{195}Pt(^{37/35}Cl)$ isotope shifts for the complexes $[Pt^{35/37}Cl_{6-n}(H_2O)_n]^{(2-n)-}$ (n = 2–6; open diamonds) and $[Pt^{35/37}Cl_{6-n}(^{16}OH)_n]^{2-}$ (n = 0–5; solid circles) at 273 K. Also plotted are the $^1\Delta^{195}Pt(^{18/16}O)$ isotope shifts for the complexes $[Pt^{35/37}Cl_{6-n}(^{16/18}OH)_n]^{2-}$ (n = 1–6; open circles).

increase in the absolute value of $^1\Delta^{195}Pt(^{18/16}O)/\delta(^{195}Pt)$ with an increasing number (n) of hydroxido ligands bound to platinum(IV) to the degree of overall deshielding of the complex anion is seen. The corresponding $^{35/37}$Cl isotope shifts of the hydroxido complexes also systematically increase as a function of the overall chemical shifts $\delta(^{195}Pt)$/ppm, although the change is larger for the intrinsic $^{16/18}$O isotope shifts. By contrast, no strong correlation is observed for both the corresponding intrinsic $^1\Delta^{195}Pt(^{37/35}Cl)$ isotope shifts for the kinetically more labile $[PtCl_{6-n}(H_2O)_n]^{(2-n)-}$($n$ = 1–5) complexes,[30] which show only a small variations with the overall extent of deshielding of the respective platinum(IV) complex.

The reasons for the observed correlations in Figure 5 are not clear currently. In the recent DFT study by Davis et al. probing isotope shifts in ^{195}Pt and ^{103}Rh NMR spectra,[46] it was generally found that the zero-point vibrationally averaged Pt–O/Cl bond displacements, as well as differences in the computed shielding/bond-length derivatives ($\partial\sigma_{Pt}/\partial r_{Pt-X}$) for the various Pt–X (X = O/Cl) bonds in various isotopologues of representative complex anions, are significant factors in accounting for the observed isotope effects for inter alia $[Pt^{35/37}Cl_{6-n}(OH)_n]^{2-}$ (n = 1–5) complexes. Intuitively, one might expect that the computed shielding/bond-length

DOI: 10.1021/ic502901d
Inorg. Chem. 2015, 54, 2752–2764

derivatives ($\partial\sigma_{Pt}/\partial r_{Pt-X}$) for the various Pt−O/Cl bonds, as a measure of relative "sensitivity" to Pt−X interatomic distances, may account for the experimentally observed trends in Figure 5. However, the gas-phase- and COSMO-model-computed $\partial\sigma_{Pt}/\partial r_{Pt-X}$ values (ppm/Å) for two representative complexes, the *cis*-$[PtCl_4(OH)_2]^{2-}$ anion compared to its uncharged aquated *cis*-$[PtCl_4(H_2O)_2]$ analogue, show that $\partial\sigma_{Pt}/\partial r_{Pt-Cl}$ calculated for the Pt−Cl bond is actually larger than that obtained for the $\partial\sigma_{Pt}/\partial r_{Pt-O}$ value, which appears counterintuitive.[46] Thus, $\partial\sigma_{Pt}/\partial r_{Pt-Cl}$ for Pt−Cl trans to a hydroxido ligand ranges from ca. −2934 to −2962 ppm/Å, compared to that for Pt−Cl cis to a coordinated OH^- ion, which ranges from −5188 to −4019 ppm/Å. By contrast, the $\partial\sigma_{Pt}/\partial r_{Pt-O}$ values obtained for the Pt−OH bonds range from −2134 to −1978 ppm/Å (the latter value determined in a polarizable continuum model COSMO). The corresponding values of $\partial\sigma_{Pt}/\partial r_{Pt-Cl}$ for the structurally identical, aquated $[PtCl_4(H_2O)_2]$ complex range from −2099 to −2370 ppm/Å for a cis to water Pt−Cl bond and −3885 to −4069 ppm/Å for a trans to water Pt−Cl bond, while the $\partial\sigma_{Pt}/\partial r_{Pt-O}$ values for a Pt−(OH_2) bond were found to be −3136 ppm/Å.[46] Nevertheless, because the isotopic resolution observed in the experimental ^{195}Pt NMR spectra depends not only on the $\partial\sigma_{Pt}/\partial r_{Pt-X}$ as calculated[46] but also on the effective Δ_{PtX} elongation/shortening in the Pt−Cl and Pt−O bond displacements trans to an OH^- ligand in a specific platinum complex anion in solution at a specific temperature, the apparent "counterintuitive" result above may not be unreasonable. Unfortunately, these DFT studies also show that fully quantitative and accurate theoretical reproduction of the experimental intrinsic $^1\Delta^{195}Pt(^{37/35}Cl)$ isotope effects in platinum(IV) complexes reported here has not yet been achieved. This may possibly be due to inter alia the importance and necessity of including more realistic microsolvation effects with many more water molecules in the second solvation shell of these complexes, as well as probably requiring a fully dynamical (CPMD or QM/MM) description in polar solvents such as water. The importance of taking into account solvation effects when probing ^{195}Pt NMR shielding in simple complex anion and the difficulty of obtaining accurate ^{195}Pt shielding constants using ab initio molecular dynamics (aiMD) calculations based on DFT have recently been demonstrated by Truflandier and Autschbach.[14]

CONCLUSIONS

Significant experimental differences in the intrinsic $^1\Delta^{195}Pt(^{37/35}Cl)$ isotope effects in the ^{195}Pt NMR profiles of the $[Pt^{35/37}Cl_{6-n}(OH)_n]^{2-}$ (n = 1−5) anions, which show only resolution at the $^{35/37}$Cl isotopologue level, have been found, resulting in (6 − n) + 1 well-resolved ^{195}Pt NMR peaks for these complexes at 293 K in high magnetic fields. This is in contrast to the previously described corresponding aquated $[PtCl_{6-n}(H_2O)_n]^{(2-n)-}$ (n = 0−5) complexes,[34,35] which also show isotopomer resolution for some of their isotopologues. These isotope-induced ^{195}Pt NMR profiles constitute unique NMR fingerprints with which to assign such species regardless of the accurate chemical shifts $\delta(^{195}Pt)$/ppm of the species. Significant $^1\Delta^{195}Pt(^{18/16}O)$ effects, which are clearly resolved at the isotopomer level for some isotopologues in ^{18}OH-enriched $[PtCl_{6-n}(OH)_n]^{2-}$ (n = 1−5), confirm the significant role that the trans influence of ligands coordinated to these platinum(IV) complexes must play in this context. Evidently, the greater trans influence of the hydroxido ligand in the order OH^- > Cl^- > H_2O in these platinum(IV) complexes results in significantly shorter Pt−OH bonds overall and, in particular, trans to coordinated chlorido ligands, so that $^{16/18}$O isotopomer-level resolution in the ^{195}Pt NMR profile of $[Pt^{35/37}Cl_{6-n}(^{16/18}OH)_n]^{2-}$ (n = 1−5) is emphasized specifically where magnetically nonequivalent isotopomers are statistically possible for these isotopologues. Nevertheless, the fact that $^{35/37}$Cl-based isotopomer effects are visible in selected species of the aquated $[Pt^{37/35}Cl_{6-n}(H_2{}^{16}O)_n]^{(2-n)-}$ (n = 0−5) complexes but not resolved in their $[Pt^{35/37}Cl_{6-n}(^{16}OH)_n]^{2-}$ (n = 1−5) counterparts can only be reasonably accounted for in terms of differences in the trans influence of H_2O and OH^- ligands. The limited data on interatomic distances available in the solid state, as discussed above for the trans fragment Cl−Pt−X (X = H_2O vs OH^-), also broadly supports this contention. Nevertheless, in the absence of more sophisticated computational work able to take into account both the effects of extensive solvation of these complexes in solution, as well as the dynamic vibrational averaging of Pt−Cl/OH/OH_2 that inevitably occurs, a more quantitative description of the significance of the trans influence of the OH^- ligand and the consequent lack of isotopomer-based intrinsic $^1\Delta^{195}Pt(^{37/35}Cl)$ isotope effects visible in the ^{195}Pt NMR profiles of the $[Pt^{35/37}Cl_{6-n}(OH)_n]^{2-}$ (n = 1−5) anions, must await further work.

ASSOCIATED CONTENT

Supporting Information

Distribution of species of the series of $[PtCl_{6-n}(OH)_n]^{2-}$ (n = 0−5) anions generated by dissolution of $Na_2[PtCl_6]\cdot 6H_2O$ in a strongly alkaline aqueous 4.0 M NaOH and monitored by 128.8 MHz ^{195}Pt NMR over time, representative additional intrinsic $^1\Delta^{195}Pt(^{37/35}Cl)$ and $^1\Delta^{195}Pt(^{18/16}O)$ isotope 128.8 MHz ^{195}Pt NMR profiles of $[Pt^{35/37}Cl_5(^{16/18}OH)]^{2-}$, *cis*-$[Pt^{35/37}Cl_4(^{16/18}OH)_2]^{2-}$, *fac*-$[Pt^{35/37}Cl_3(^{16/18}OH)_3]^{2-}$, and $[Pt(^{16/18}OH)_6]^{2-}$, and table listing the comparison of experimental and statistically expected intrinsic $^1\Delta^{195}Pt(^{37/35}Cl)$ and $^1\Delta^{195}Pt(^{18/16}O)$ isotope profiles of $[Pt^{35/37}Cl_5(^{16/18}OH)]^{2-}$, *cis*-$[Pt^{35/37}Cl_4(^{16/18}OH)_2]^{2-}$, *fac*-$[Pt^{35/37}Cl_3(^{16/18}OH)_3]^{2-}$, $[Pt^{35/37}Cl(^{16/18}OH)_5]^{2-}$, and $[Pt(^{16/18}OH)_6]^{2-}$ species. This material is available free of charge via the Internet at http://pubs.acs.org.

AUTHOR INFORMATION

Corresponding Author

*E-mail: krk@sun.ac.za. Tel: 002721 8083020. Fax: 002721 808 2342.

Notes

The authors declare no competing financial interest.

ACKNOWLEDGMENTS

Financial support from the National Research Foundation (Incentive Funding and Innovation bursary to L.E.), Stellenbosch University, and Angloplatinum Ltd. is gratefully acknowledged.

REFERENCES

(1) Proctor, W. G.; Yu, F. C. *Phys. Rev.* **1951**, *81*, 20−30.
(2) Harris, R. K.; Becker, E. D.; Cabral De Menezes, S. M.; Goodfellow, R.; Granger, P. *Pure Appl. Chem.* **2001**, *73*, 1795−1818.
(3) Pregosin, P. S. *Coord. Chem. Rev.* **1982**, *44*, 247−291.
(4) Priqueler, J. R. L.; Butler, I. S.; Rochon, F. D. *Appl. Spectrosc. Rev.* **2006**, *41*, 185−226.
(5) Pregosin, P. S. *Annu. Rep. NMR Spectrosc.* **1986**, *17*, 285−349.

DOI: 10.1021/ic502901d
Inorg. Chem. 2015, 54, 2752−2764

(6) Still, B. M.; Kumar, P. G. A.; Aldrich-Wright, J. R.; Price, W. S. *Chem. Soc. Rev.* **2007**, *36*, 665−686.
(7) Chen, W.; Liu, F.; Matsumoto, K.; Autschbach, J.; Le Guennic, B.; Ziegler, T.; Maliarik, M.; Glaser, J. *Inorg. Chem.* **2006**, *45*, 4526−4536.
(8) Dean, R. R.; Green, J. C. *J. Chem. Soc. A* **1968**, 3047−3050.
(9) Gilbert, T. M.; Ziegler, T. *J. Phys. Chem. A* **1999**, *103*, 7535−7543.
(10) Sterzel, M.; Autschbach, J. *Inorg. Chem.* **2006**, *45*, 3316−3324.
(11) Bühl, M.; Mauschick, F. T.; Terstegen, F.; Wrackmeyer, B. *Angew. Chem., Int. Ed.* **2002**, *41*, 2312−2315.
(12) Bühl, M.; Mauschick, F. T. *Phys. Chem. Chem. Phys.* **2002**, *4*, 5508−5514.
(13) Bühl, M.; Grigoleit, S.; Kabrede, H.; Mauschick, F. T. *Chem.—Eur. J.* **2005**, *12*, 477−488.
(14) Truflandier, L. A.; Autschbach, J. *J. Am. Chem. Soc.* **2010**, *132*, 3472−3483.
(15) Pesek, J. J.; Mason, W. R. *J. Magn. Reson.* **1977**, *25*, 519−529.
(16) Cohen, S. M.; Brown, T. H. *J. Chem. Phys.* **1974**, *61*, 2985−2986.
(17) Ismail, I. M.; Kerrison, S. J. S.; Sadler, P. J. *J. Chem. Soc., Chem. Commun.* **1980**, 1175−1176.
(18) Gröning, Ö.; Elding, L. I. *Inorg. Chem.* **1989**, *28*, 3366−3372.
(19) Wrackmeyer, B.; Klimkina, E. V.; Schmalz, T.; Milius, W. *Magn. Reson. Chem.* **2013**, *51*, 283−291.
(20) Ramsey, N. F. *Phys. Rev.* **1952**, *87*, 1075−1079.
(21) Gombler, W. *J. Am. Chem. Soc.* **1982**, *104*, 6616−6620.
(22) (a) Batiz-Hernandez, H.; Bernheim, R. A. *Prog. Nucl. Reson.* **1967**, *3*, 63−85. (b) Hansen, P. E. *Annu. Rep. NMR Spectrosc.* **1984**, *15*, 105−234. (c) Hansen, P. E. *Prog. Nucl. Magn. Reson.* **1988**, *20*, 207−255.
(23) (a) Kerschl, S.; Sebald, A.; Wrackmeyer, B. *Magn. Reson. Chem.* **1985**, *23*, 514−520. (b) Sebald, A.; Wrackmeyer, B. *J. Magn. Reson.* **1985**, *63*, 397−400.
(24) Anet, F. A. L.; Dekmezian, A. H. *J. Am. Chem. Soc.* **1979**, *101*, 5449−5451.
(25) Stringfellow, T. C.; Wu, G.; Wasylishen, R. E. *J. Phys. Chem. B* **1997**, *101*, 9651−9656.
(26) Kramer, J.; Koch, K. R. *Inorg. Chem.* **2006**, *45*, 7843−7855.
(27) Kramer, J.; Koch, K. R. *Inorg. Chem.* **2007**, *46*, 7466−7476.
(28) Koch, K. R.; Burger, M. R.; Kramer, J.; Westra, A. N. *Dalton Trans.* **2006**, 3277−3284.
(29) Gerber, W. J.; Murray, P.; Koch, K. R. *Dalton Trans.* **2008**, 4113−4117.
(30) Murray, P.; Gerber, W. J.; Koch, K. R. *Dalton Trans.* **2012**, *41*, 10533−10542.
(31) Geswindt, T. E.; Gerber, W. J.; Brand, D. J.; Koch, K. R. *Anal. Chim. Acta* **2012**, *730*, 93−98.
(32) Carr, C.; Goggin, P. L.; Goodfellow, R. J. *Inorg. Chim. Acta* **1984**, *81*, L25−L26.
(33) Appleton, T. G.; Hall, J. R.; Ralph, S. F. *Inorg. Chem.* **1985**, *24*, 4685−4693.
(34) *MestReNova 7.1.1*; Mestrelab Research SL: Santiago de Compostela, Spain, 2012
(35) Gee, M.; Wasylishen, R. E.; Laaksonen, A. *J. Phys. Chem. A* **1999**, *103*, 10805−10812.
(36) Preetz, W.; Peters, G.; Bublitz, D. *Chem. Rev.* **1996**, *96*, 977−1025.
(37) Jameson, C. J. *J. Chem. Phys.* **1977**, *66*, 4983−4988.
(38) (a) Jameson, C. J.; Osten, H.-J. *J. Chem. Phys.* **1984**, *81*, 4293; (b) *Annu. Rep. NMR Spectrosc.* **1986**, *17*, 1−78.
(39) Jameson, C. J.; Jameson, A. K. *J. Chem. Phys.* **1986**, *85*, 5484−5492.
(40) Jameson, C. J. *Annu. Rev. Phys. Chem.* **1996**, *47*, 135−69.
(41) Jameson, C. J.; Jameson, A. K.; Oppusunggu, D. *J. Chem. Phys.* **1986**, *85*, 5480−5483.
(42) Jameson, C. J.; Rehder, D.; Hoch, M. *J. Am. Chem. Soc.* **1987**, *109*, 2589−2594.
(43) Penka Fowe, E.; Belser, P.; Daul, C.; Chermette, H. *Phys. Chem. Chem. Phys.* **2005**, *7*, 1732.
(44) Burger, M. R.; Kramer, J.; Chermette, H.; Koch, K. R. *Magn. Reson. Chem.* **2010**, *48* (S1), S38−S47.
(45) Davis, J. C.; Bühl, M.; Koch, K. R. *J. Chem. Theory Comput.* **2012**, *8*, 1344−1350.
(46) Davis, J. C.; Bühl, M.; Koch, K. R. *J. Phys. Chem. A* **2013**, *117*, 8054−8064.
(47) Bondar, V. I.; Potekhin, K. A.; Rau, T. F.; Rozman, S. P.; Rau, V. G.; Struchkov, Y. T. *Sov. Phys. Dokl.* **1988**, *33*, 395−396.
(48) Steinborn, D.; Gravenhorst, O.; Hartung, H.; Baumeister, U. *Inorg. Chem.* **1997**, *36*, 2195−2199.
(49) Dunham, S. U.; Abbott, E. H. *Inorg. Chim. Acta* **2000**, *297*, 72−78.
(50) Dechter, J. J.; Kowalewski, J. *J. Magn. Reson.* **1984**, *59*, 146−149.

DOI: 10.1021/ic502901d
Inorg. Chem. 2015, 54, 2752−2764